

5-1-2019

# COMPARISON OF STRENGTH, DUCTILITY AND STIFFNESS FOR RADIUS CUT AND STRAIGHT CUT OF REDUCED BEAM SECTION

Venkat Ramana Reddy Vootukuri

*Southern Illinois University Carbondale*, [ramana.vootukuri@gmail.com](mailto:ramana.vootukuri@gmail.com)

Follow this and additional works at: <https://opensiuc.lib.siu.edu/theses>

---

## Recommended Citation

Vootukuri, Venkat Ramana Reddy, "COMPARISON OF STRENGTH, DUCTILITY AND STIFFNESS FOR RADIUS CUT AND STRAIGHT CUT OF REDUCED BEAM SECTION" (2019). *Theses*. 2536.

<https://opensiuc.lib.siu.edu/theses/2536>

This Open Access Thesis is brought to you for free and open access by the Theses and Dissertations at OpenSIUC. It has been accepted for inclusion in Theses by an authorized administrator of OpenSIUC. For more information, please contact [opensiuc@lib.siu.edu](mailto:opensiuc@lib.siu.edu).

COMPARISON OF STRENGTH, DUCTILITY AND STIFFNESS FOR RADIUS CUT  
AND STRAIGHT CUT OF REDUCED BEAM SECTION

by

Venkat Ramana Reddy Vootukuri

B. Tech, Gokaraju Rangaraju Institute of Engineering and Technology, 2016

A Thesis

Submitted in Partial Fulfillment of the Requirements for the  
Master of Science Degree

Department of Civil and Environmental Engineering  
in the Graduate School  
Southern Illinois University Carbondale  
May 2019

THESIS APPROVAL

COMPARISON OF STRENGTH, DUCTILITY AND STIFFNESS FOR RADIUS CUT  
AND STRAIGHT CUT OF REDUCED BEAM SECTION

By

Venkat Ramana Reddy Vootukuri

A Thesis Submitted in Partial

Fulfillment of the Requirements

for the Degree of

Master of Science

in the field of Civil and Environmental Engineering

Approved by:

Dr. J. Kent Hsiao, Chair

Dr. Aslam Kassimali

Dr. Jale Tezcan

Graduate School  
Southern Illinois University Carbondale  
February 27, 2019

## AN ABSTRACT OF THE THESIS OF

VENKAT RAMANA REDDY VOOTUKURI, for the Master of Science degree in CIVIL ENGINEERING, presented on February 27, 2018, at Southern Illinois University Carbondale.

TITLE: COMPARISON OF STRENGTH, DUCTILITY AND STIFFNESS FOR RADIUS CUT AND STRAIGHT CUT OF REDUCED BEAM SECTION

MAJOR PROFESSOR: Dr. J. Kent Hsiao, Ph.D., P.E.(CA), S.E.(UT)

In 1994 there was an earthquake occurred in Northridge, California which caused damage in structures built with Steel Moment Frames due to the brittle fractures in the beam and column connections. It has led to the major modifications and improvements in the connection detailing after to the earthquake occurred in the Northridge. These changes came up with better materials for welding and introduced the use of cover plate and Reduced Beam Section (RBS). RBS connections are the most widely used connection today and it allows the Steel Moment Frame systems to yield extensively and deform plastically by avoiding brittle fracturing at connections. The most important factors that affect the response along with the design of Steel Moment Frames and Reduced Beam Section (RBS) connections are connection stiffness, ductility, connection type, and strength of the column.

The purpose of this research is to investigate the Strength, Ductility, and Stiffness between the two distinct types of Reduced Beam Section Connections with same sectional and material properties by using finite element analysis. In this research two sets of finite element models were designed by assuming that the point of inflection occurs at the mid span of beam and mid-height of each story column, so half beam half column configuration was considered for the analysis in which one is for Reduced Beam Section - Radius Cut and another is for Reduced Beam Section - Straight Cut. Each

section of column and beam were designed in the initial stage by using RBS connections design recommendations from The Federal Emergency Management Agency FEMA-350 (FEMA 350, 2000) and then modeled and analyzed by using finite element analysis software. Results were computed and comparisons were made with respect to the location of the plastic hinge. For each model strengths obtained from the hand calculations were compared with strengths obtained from the finite element analysis.

The Connections were designed using FEMA 350 - Recommended Seismic Design Criteria for New Steel Moment-Frame Buildings along with AISC steel construction manual (AISC, 2012). For all the model's non-linear analysis was performed by using finite element analysis. Comparisons were made based on the computed results in terms of ductility, strength, and stiffness. For each model strengths obtained from finite element analysis were compared with hand calculations

## ACKNOWLEDGEMENTS

I am using this opportunity to express my deepest appreciation to all who, directly and indirectly, have lent their helping hands in finishing my thesis. First and foremost, I would like to express my sincere gratitude to my academic advisor, role model, mentor Dr. J. Kent Hsiao, for his continuous support, consistence patience, encouragement, outstanding teaching, and guidance for my thesis and graduate classes. I appreciate all the time he spent on enlightening me and tireless answering all my questions, his tremendous advice has helped me progress significantly from data collection, analysis to the research writing.

Besides my advisor, I would like to thank my seniors Dr. Akwasi Assenso Antwi and Dr. Alex Yunyi Jiang and my friend Frederick Mensah for sharing all their knowledge regarding finite element computer analysis (NISA) and for being a big help for the completion of my thesis. Thank you for always being encouraging, positive and aspiring guidance throughout the whole year.

I would also like to thank Dr. Aslam Kassimali and Dr. Jale Tezcan for being part of my graduate committee. Thank you both for your excellent teaching throughout my graduate classes and also for your insightful comments by reviewing my work. I feel humbled that I would be able to work and collaborate with great researchers.

I express my deepest thanks to the Civil Engineering Department and my chair Dr. Sanjeev Kumar for the continuous support both in academically and financially to pursue my master's studies, for his motivation, enthusiasm, and immense knowledge. Without his support and persistent help, I couldn't have imagined me getting my

master's degree from SIUC. I choose this moment to acknowledge his contribution gratefully.

Last but not the least, I am sincerely grateful to all my family members, mother (Anitha Reddy), father (Karunakar Reddy), sister (Vyshnavi Reddy), grandparents and my friends for their unconditional love, eternal encouragement, care and their support throughout my research and my life in general. I would not have been able to complete this thesis dissertation without their continuous support and encouragement.

Venkat Ramana Reddy, Vootukuri

*Carbondale, Illinois*  
*February 2019*

## TABLE OF CONTENTS

<u>CHAPTER</u>	<u>PAGE</u>
ABSTRACT .....	i
ACKNOWLEDGEMENTS .....	iii
LIST OF TABLES .....	vii
LIST OF FIGURES .....	viii
CHAPTERS	
CHAPTER 1 – INTRODUCTION .....	1
CHAPTER 2 – LITERATURE REVIEW .....	4
2.1 Background of Steel Moment Frames .....	4
2.2 Steel Moment Frames .....	4
2.3 Formation of Plastic Hinge.....	6
2.4 Reduced Beam Section Connection (RBS) .....	8
2.5 First Principal Stress and Von-Mises Stress.....	10
CHAPTER 3 – FINITE ELEMENT MODELLING .....	11
3.1 Introduction .....	11
3.2 Geometry of the Model .....	15
3.3 Material Properties .....	17
3.4 Loads and Boundary Conditions.....	18
3.5 Finite Element Analysis .....	19
CHAPTER 4 – RESULTS AND DISCUSSION .....	20
4.1 Brief Introduction .....	20
4.2 Outputs from Finite Element Analysis Software.....	21

4.3 Stresses, Plastic Hinge Formation and Strength .....	22
4.3.1 Reduced Beam Section – Radius Cut .....	22
4.3.2 Reduced Beam Section – Straight Cut .....	29
4.4 Lateral Load Applied on the Models .....	35
4.4.1 Lateral Load when 1st Principal Stress is at 84 ksi.....	36
4.4.2 Lateral Load when Von-Mises Stress Reaches at 57 ksi.....	37
4.5 Displacement and Ductility .....	37
4.5.1 Lateral Displacement when 1st Principal Stress Reaches at 84 ksi.....	38
4.5.2 Lateral Displacement when Von-Mises Stress is at 57 ksi .....	38
4.5.3 Comparison and Computations of Ductility.....	39
4.6 Stiffness.....	40
4.6.1 Comparison and Computation of Stiffness .....	41
CHAPTER 5 – SUMMARY AND COMPARISON OF RESULTS.....	43
CHAPTER 6 – CONCLUSION.....	45
REFERENCES.....	47
APPENDICES	
APPENDIX A (DESIGN PROCEDURE).....	49
VITA .....	62

## LIST OF TABLES

<u>TABLE</u>		<u>PAGE</u>
Table 3.3.1	True Stress vs. Strain Data for A992 Steel.....	18
Table 4.4.1.1	Lateral Load Calculations when 1st Principal Stress Reaches 84 ksi ....	36
Table 4.4.2.1	Lateral Load Calculations when Von-Mises Stress Reaches 57 ksi .....	37
Table 4.5.1.1	Lateral Displacements when 1st Principal Stress Reaches 84 ksi .....	38
Table 4.5.2.1	Lateral Displacements when Von-Mises Stress Reaches 57 ksi.....	38
Table 4.5.3.1	Calculations for Ductility Ratio.....	39
Table 4.5.3.2	Comparison of Ductility Ratio .....	40
Table 4.6.1	Lateral Displacement and Lateral Load when Von-Mises Stress Reaches 57 ksi .....	40
Table 4.6.1.1	Stiffness Computations and Comparison (Elastic Range).....	42
Table 5.1	Comparison and Summary of Results Recorded from the Outputs of NISA 2010.....	43
Table 5.2	Comparison of Strengths Obtained from Finite Element Analysis and Hand Calculations .....	44
Table A.1	Section Properties for the Beam and Column for both Models .....	49

## LIST OF FIGURES

<u>FIGURE</u>	<u>PAGE</u>
Figure 1.1 RBS Straight Cut, Tapered Cut and Radius Cut .....	3
Figure 2.2.1 Typical Moment Resisting Frame .....	6
Figure 2.3.1 Single Story Mechanism (Krawinkler et.al 2009).....	7
Figure 2.4.1 Typical Layout of Reduced Beam Section Connection as per FEMA 350 .....	9
Figure 2.4.2 Typical Reduced Beam Section Connection .....	9
Figure 3.1.1 Half Beam - Half Column Configuration from a Two Bay and Two-Story frame .....	11
Figure 3.1.2 Typical Model Configuration of RBS Connection .....	12
Figure 3.1.3 Typical Model Configuration of RBS Connection along with Loading .....	13
Figure 3.1.4 Typical Model Configuration for Steel Moment Frames using RBS Connection with Loading .....	14
Figure 3.1.5 Isometric View of Typical Model Configuration using RBS Connection .....	14
Figure 3.2.1 Model 1, RBS Straight Cut Connection .....	15
Figure 3.2.2 Model 2, RBS Radius Cut Connection .....	16
Figure 3.3.1 A True Stress vs. Strain Curve for A992 Steel .....	17
Figure 3.4.1 Typical Distribution of Lateral Load Applied on the Top Plate of the Column.....	19
Figure 4.1.1 Beginning of the Formation of Plastic Hinge on RBS .....	21

Figure 4.3.1.1	Reduced Beam Section – Radius cut plan view.....	22
Figure 4.3.1.2	Reduced Beam Section – Radius Cut Isometric View.....	22
Figure 4.3.1.3	The 1st Principal Stress at 84 ksi (RBS – Radius Cut Model).....	23
Figure 4.3.1.4	Von-Mises Stress at 57 ksi (RBS – Radius Cut Model).....	24
Figure 4.3.1.5	Lateral Displacement when 1st Principal Stress is at 84 ksi (RBS – Radius Cut Model) .....	25
Figure 4.3.1.6	Lateral Displacement when Von-Mises Stress is at 57 ksi (RBS – Radius Cut Model) .....	26
Figure 4.3.1.7	Von-Mises Stress Distribution (RBS – Radius Cut Model).....	27
Figure 4.3.1.8	Final Plastic Hinge Formation (RBS – Radius Cut Model) .....	28
Figure 4.3.2.1	Reduced Beam Section – Straight Cut Plan View.....	29
Figure 4.3.2.2	Reduced Beam Section – Straight Cut Isometric View.....	29
Figure 4.3.2.3	1st Principal Stress at 84 ksi (RBS – Straight Cut Model).....	30
Figure 4.3.2.4	Von-Mises Stress at 57 ksi (RBS – Straight Cut Model).....	31
Figure 4.3.2.5	Lateral Displacement when 1st Principal Stress is at 84 ksi (RBS – Straight Cut Model).....	32
Figure 4.3.2.6	Lateral Displacement when Von-Mises Stress is at 57 ksi (RBS – Straight Cut Model).....	33
Figure 4.3.2.7	Von-Mises Stress Distribution (RBS – Straight Cut Model).....	34
Figure 4.3.2.8	Final Plastic Hinge Formation (RBS – Straight Cut Model) .....	35
Figure 4.6.1.1	Overlap of RBS – Straight Cut and Radius Cut.....	41
Figure A1	Dimensions of a W section .....	49
Figure A2	Reduced Beam Section Connection (Radius Cut).....	50

Figure A3	Plastic Hinge Formation for RBS .....	52
Figure A4	Calculation of Moments at Critical Sections.....	55
Figure A5	Calculation of Section Modulus for RBS .....	57

## CHAPTER 1

### INTRODUCTION

The impact of two major earthquakes that were occurred in Northridge, California on (January 17<sup>th</sup>, 1994 LA) and Kobe, Hyōgo on (January 17, 1995 Japan) were so disastrous which in turn affected the design codes for Steel Moment Frame connections that were used before these earthquakes, these code books had to be modified / revised. The investigation has been done by (Hwang et al., 2009) and noted the observations of brittle fractures in the beam and column connections FEMA-350 (FEMA 350, 2000), which was failed at much lower condition of the load than estimated load. The main lesson that was learned from Northridge earthquake is the potential deficiency of beam column joints in moment resisting frames (Tremblay et al., 1995).

After the earthquake, the wide range of research was held to find out the most accurate solutions to the issues that were occurred, to prevent from the damage that's going to occur in future. Over the last 20 years the construction industries and the design professionals has come up together for the review and to revise the different factors involved in the steel moment frame construction. From the research it was proved that there were several factors which was causing problems and deficiency in moment resisting frames and which in result caused a failure in the Steel Moment Frame structures due to Northridge Earthquake. There were some important factors that resulted in formation of higher stress concentrations and propagated local failures around the connections, they are inadequate detailing, poor welding practices and procedures used for designing (Mao et al., 2001). Different researches were carried out by AISC in collaboration with structural organizations and led to the FEMA-SAC

program on the improvements in fabrication, workmanship, and design which were expected to raise the performance of the Steel Moment Frames (Chen et al., 1996).

For an effective seismic performance, it is important to provide the link with adequate stiffness, ductility and strength. The location of the plastic hinge where ductile failure occurs can be made to occur away from the column, for this failure to occur away from the column there are many methods that can change the location of the failure. Out of which there are two major methods that are considered by (Shi et al., 2012), one of the methods which eliminates high stress concentration at column-beam interface is by reducing the area of the beam at a certain distance which is known as reduced beam section connection and another method is welded flange plate connections which involves increasing the thickness of the beam flanges at the face of the column which can be made by adding cover plates to top and bottom flange of the beam at face of the column.

There are three types of RBS with different flange reduction conditions, Figure 1.1 shows the Reduced beam section Straight Cut, Tapered Cut and Radius Cut respectively. Reduced beam section connection protects the column-beam interface by forcing the occurrence of plastic hinge to form at a certain distance away from the face of column within the reduced beam section, this kind of connection requires strong column and weak beam combination.

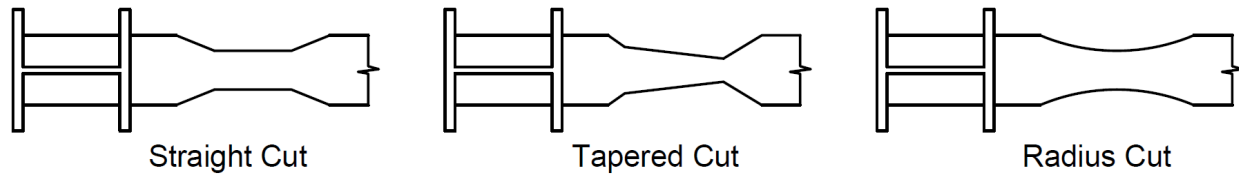


Figure 1.1 RBS Straight Cut, Tapered Cut and Radius Cut

This study focuses on the comparison of strength, ductility, and stiffness between two steel moment connections, Reduced beam section Radius Cut and Straight Cut. From a two story and two bay steel moment frames, an exterior column and beam connection at the first story was considered and designed for a half beam and half column configuration for two different types of connections with same beam and column sections were selected for two models. These two connections are designed according to the procedure provided in the FEMA 350 - Recommended Seismic Design Criteria for New Steel Moment-Frame Buildings. Finite element software NISA DISPLAY IV (NISA 2010) is used to perform modelling and analysis for RBS Radius Cut and RBS Straight Cut. Each model was first designed, modeled and then analyzed for RBS connections as per design guidelines. All the boundary conditions and loads were kept typical for all the two models. Strength, ductility and stiffness were then calculated for each model and the results were compared and summarized.

## CHAPTER 2

### LITERATURE REVIEW

#### 2.1 Background of Steel Moment Frames

Several researches were done on finding out about the factors that caused the failure of the steel moment frames. It has also proved that during the earthquake the connection's plastic hinge was formed at an undesirable location which in result caused the weld to fracture without yielding. Therefore, it is important for the moment frame connections to avoid the brittle failure of the column-beam connections by forcing the plastic hinge away from the face of the column FEMA 350 and reducing the stress levels in the surrounding areas of the joints.

Based on this, the Federal Emergency Management Agency has developed a Recommended Seismic Design Criteria for New Steel Moment-Frame Buildings - FEMA 350. This criterion has a step by step procedure for the design of different seismic connections to make sure that all the new steel moment frames will be able to handle the desired level of earthquake hazards (Roeder et al., 2002).

#### 2.2 Steel Moment Frames

During 19<sup>th</sup> century the steel frame structures were developed for the limitations of masonry bearing wall structures, which was a common mode of construction (McEntee, 2009). For construction of high-rise structures, it was difficult to build with masonry bearing wall structures, so they started using rigid frames or moment frames to build high rise structures. Steel Moment Frames were used in construction of the Home

Insurance Building of 10-storey in Chicago with a height of 138 ft is also called as skyscraper at that time (Hamburger et al., 2009). Moment resisting frames are more expensive than others, such as braced frames or shear walls, the reason is mainly because of the beam and column sizes will be heavier per linear foot and doubler plates might be required in the web of the column and it may also be required for more welding to acquire more strength.

Steel Moment Frames contains a system of beams and columns which are rigidly connected to one another either by bolting or welding (Popov et al., 1998). In Steel Moment Frames, beam to column connection plays a major role because seismic loads are resisted by the flexure action in columns and beams which cause moment as well as shears in the frames. Steel Moment Frames are typically recommended for high seismic zones.

There are three types of steel moment frames: Ordinary Moment Frames (OMF), Special Moment Frames(SMF) and Intermediate Moment Frames (IMF). As per FEMA 350, Special Moment Frames are more ductile when compared to OMF and IMF, so it is recommended to use Special Moment Frames in high seismic zones (Hernandez, 2016). OMF was typically used in non-seismic regions and they were expected to hold limited inelastic deformation in the frame elements. IMF is almost same as OMF, but it requires to use of pre-qualified connections as per AISC (AISC, 2012). In Special Moment Frames, plastic deformations and yielding is observed in the structural members while maintain structural integrity. From the different types of connections recommended by FEMA 350, this study is focused only on Reduced Beam Section. It is assumed that the point of inflection occurs at the mid-span of the beam and mid height

of the story column, so half column and half beam are used in the modelling and these are obtained from the typical Moment Resisting Frame as shown in Figure 2.2.1.

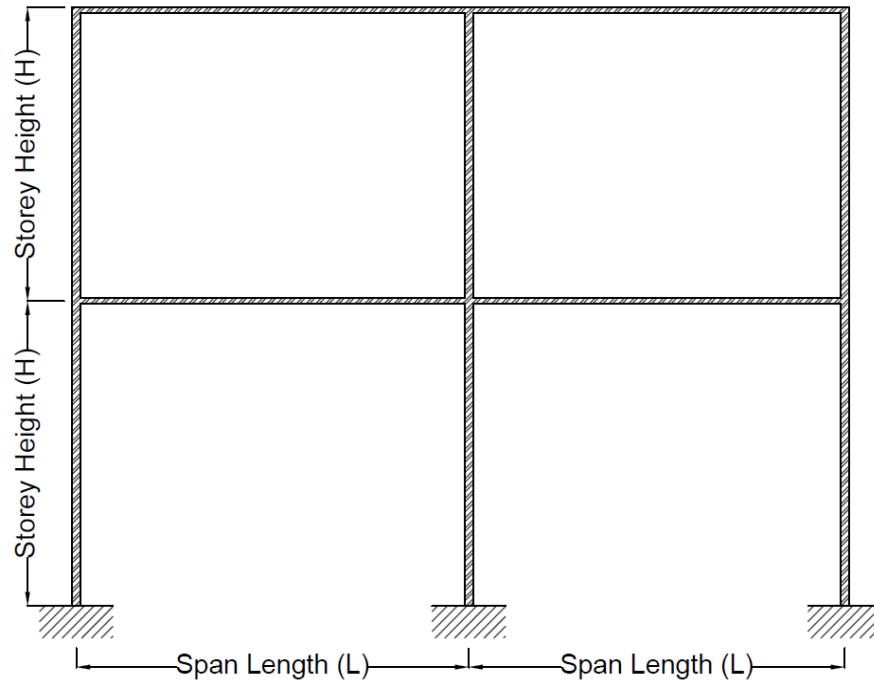


Figure 2.2.1 Typical Moment Resisting Frame

### 2.3 Formation of Plastic Hinge

Plastic Hinge is a yielding zone in a structural element which generally develops at the point of Maximum Bending Moment. It also refers to the deformation of the part of a beam wherever plastic bending happens. Investigations that were done on earthquake occurred in Northridge proved that plastic hinge was formed at undesired locations in the steel moment frames which includes face and panel zone of the column, by causing a reduction in the ductile behavior of the connection. The formation of plastic hinge in columns is undesirable which may lead in the formation of mechanisms with

the participation of few elements called as story mechanism FEMA 350. To minimize the undesirable effects of high axial loads on single story mechanisms, it is important to keep the plastic hinge away from the columns. Figure 2.3.1 shows the formation of plastic hinge in single story mechanism at column ends (Hamburger et al., 2009).

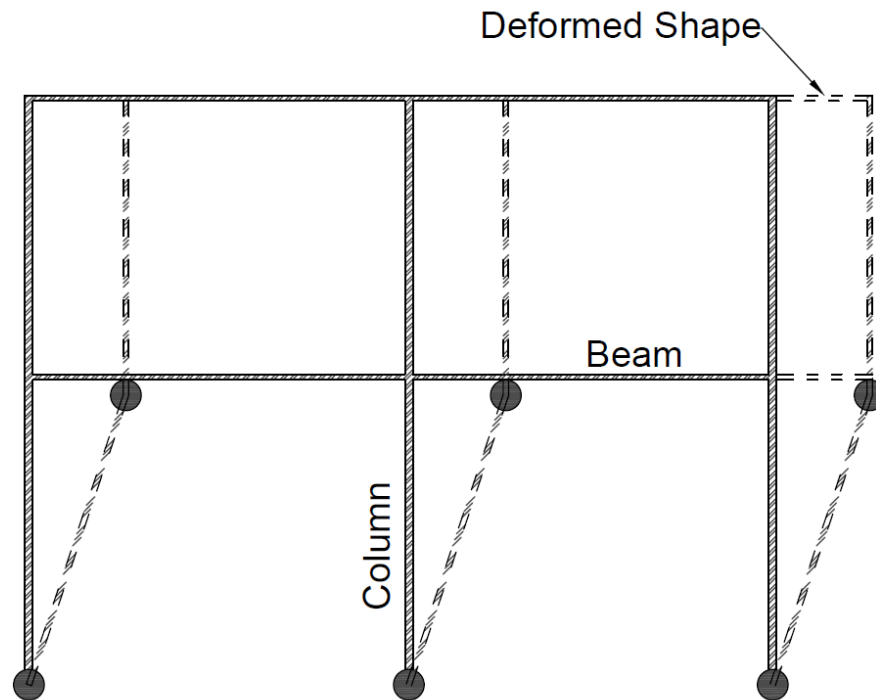


Figure 2.3.1 Single Story Mechanism (Hamburger et al., 2009)

There could be a high chance of increase in inelastic strain demands on the connection, if the plastic hinge is formed at the face of the column in beam. These conditions might drive to the brittle failure of connections, so as to avoid these kinds of failures, it is important to use the strong-column and weak-beam configuration. It is also very important to give a fully restrained column-beam connection which will ensure to force the plastic hinge location away from the face of the column, it can be achieved by reducing the cross sections of the beam flanges (RBS Connection).

## 2.4 Reduced Beam Section Connection (RBS)

The European researcher Plumier has developed an idea of forming a locally weak zone away from the column-beam connection so that the formation of the plastic hinge can occur at the desired location by utilizing the concept of reduced beam section. A lot of research (Tsavdaridis et al., 2014) has taken place so as to study the most accurate shape of reduced beam section but most of the investigations were concentrated on comparing the results from different geometrical shapes of reduced beam sections, which were divided in to three shapes namely, straight cut, tapered cut, and radius cut as shown in Figure 1.1. In all the types of reduced beam sections it uses the concept of reducing the area of beam flanges near to the column-beam connection, by this reduction of area from beam flanges further improve the ductility of the connection.

The main reason for Reduced Beam Section connections to be popular is, they don't require any additional reinforcement and that's why they are widely accepted in United States (Mirza, 2014). All the models of reduced beam section connections used in this study were designed using FEMA 350 and sectional properties for beam and column are considered same for all the models. In detail, for this type of connection system, the procedure and guidelines are provided in section 3.5.5, FEMA 350. The typical layout of Reduced Beam Section Connection as per FEMA 350 is showed in Figure 2.4.1 and Typical Reduced Beam Section Connection is shown in Figure 2.4.2

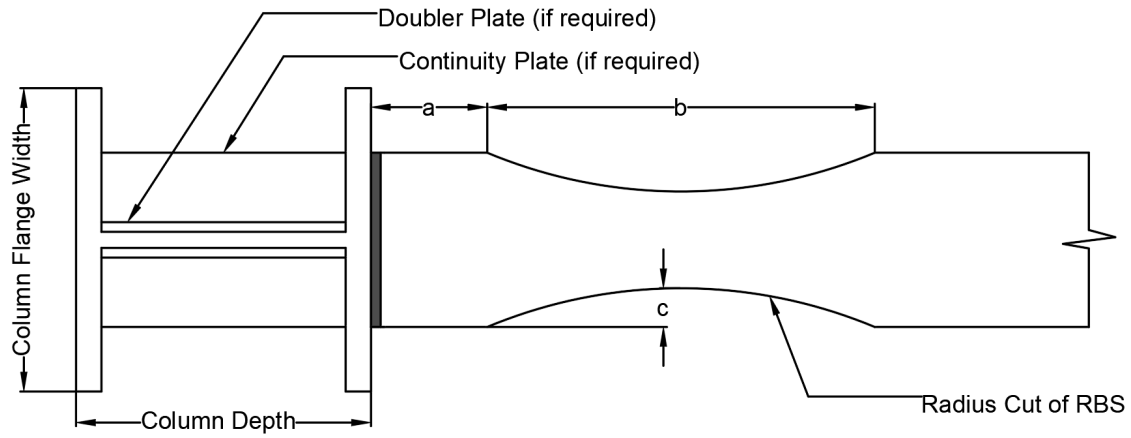


Figure 2.4.1 Typical layout of Reduced Beam Section Connection as per FEMA 350



Figure 2.4.2 Typical Reduced Beam Section Connection

## 2.5 First Principal Stress and Von-Mises Stress

From the finite element analysis that's considered material and geometric non-linearity the stress at which fracture occurs is called first principal stress, since A992 steel is used in this study the ultimate stress ( $F_u$ ) for A992 Steel is 84 ksi any result with a stress distribution higher than 84 ksi is taken as unreliable because the fracture starts occurring from this point. The strength attained at first principal stress is called as ultimate strength.

The Von-Mises yield criteria states that the when von-mises stress exceeds the yield strength, yielding start's occurring. The yield stress for A992 steel is 57 ksi (Mirza, 2014) therefore once the material has attained its yield stress 57 ksi it is assumed to be yielded. So, when Von-Mises stress reaches the stress of 57 ksi (Yield Stress = 57 ksi) then we predict that yield has been occurred.

## CHAPTER 3

### FINITE ELEMENT MODELLING

#### 3.1 Introduction

In this study a one bay and two-story Steel Moment Frame was considered and selected an exterior beam and column connection in the first story as shown in Figure 3.1.1. Both the Reduced Beam Section – Radius Cut and Reduced Beam Section – Straight Cut models were developed by considering half column and half beam configurations and also by assuming that the point of inflection occurs at the mid-span of the beam and mid height of the story column, for considering a clear analysis of concentration of stresses at the connections and also to locate the plastic hinge so that it can be seen clearly using Von-Mises stresses. While modelling of two different connections it is important to pay attention to the input values and parameters used for the analysis to make sure that models are developed accurately.

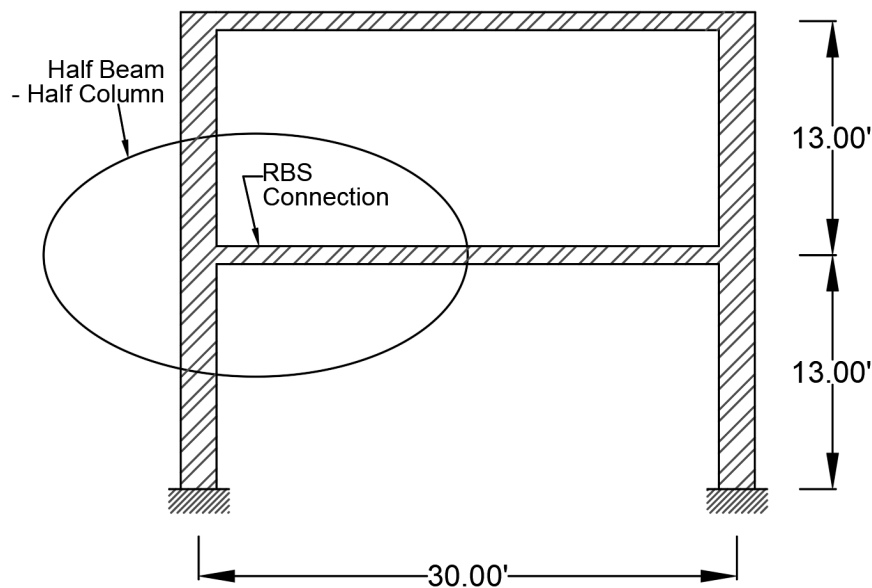


Figure 3.1.1 Half Beam - Half Column Configuration from a one bay and two-story frame

This chapter focused on explaining in detail about the material properties, construction of model and number of time steps performed for the Finite Element Analysis.

Lateral load, load direction, boundary conditions, column height, span length, section properties is used same for both the models. Lateral Load is applied on the top of column in form of pressure load and vertical loading is neglected for both the models. Referring to Figure 3.1.1, assume that the point of inflection occurs at the mid-span of the beam and mid height of the story column due to lateral load. Therefore the moments at the mid height of the column and at the mid span of the beam are considered to be zero due to lateral load. So as a boundary condition, at the bottom of the mid height of the column a pin is assumed and at the mid span of the beam a roller is assumed, and a free end is used at the top of the mid height of column.

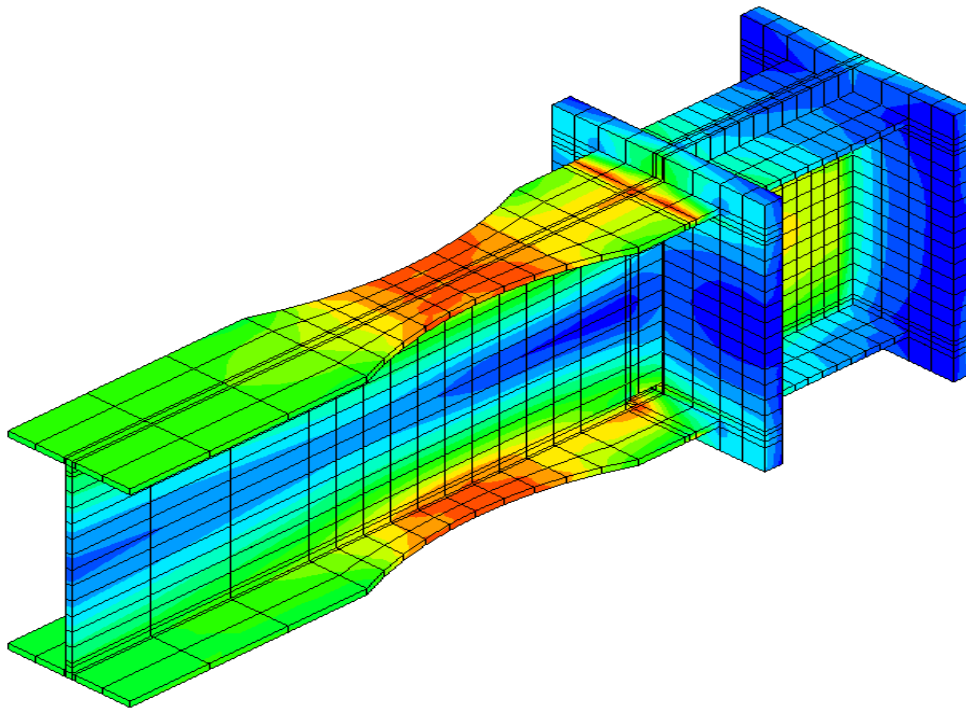


Figure 3.1.2 Typical Model Configuration of RBS Connection

A typical model configuration of RBS Connection is shown in Figure 3.1.2, a typical configuration of the RBS model with a loading condition is shown in Figure 3.1.3, and Figure 3.1.4 represents the typical Configuration for Steel Moment Frame using RBS Connection with loading and isometric view of typical model configuration for RBS connection is shown in Figure 3.1.5

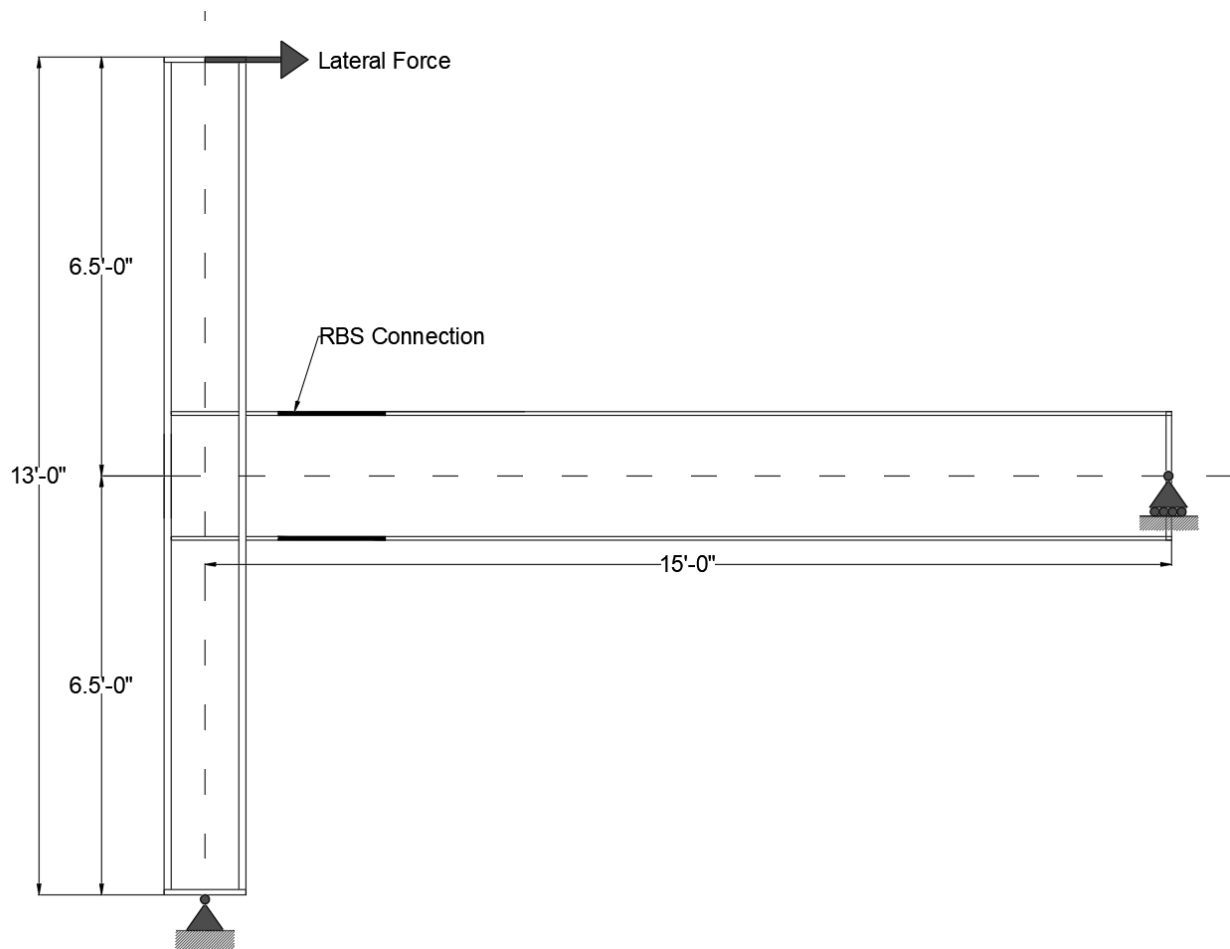


Figure 3.1.3 Typical Model Configuration of RBS Connection along with Loading

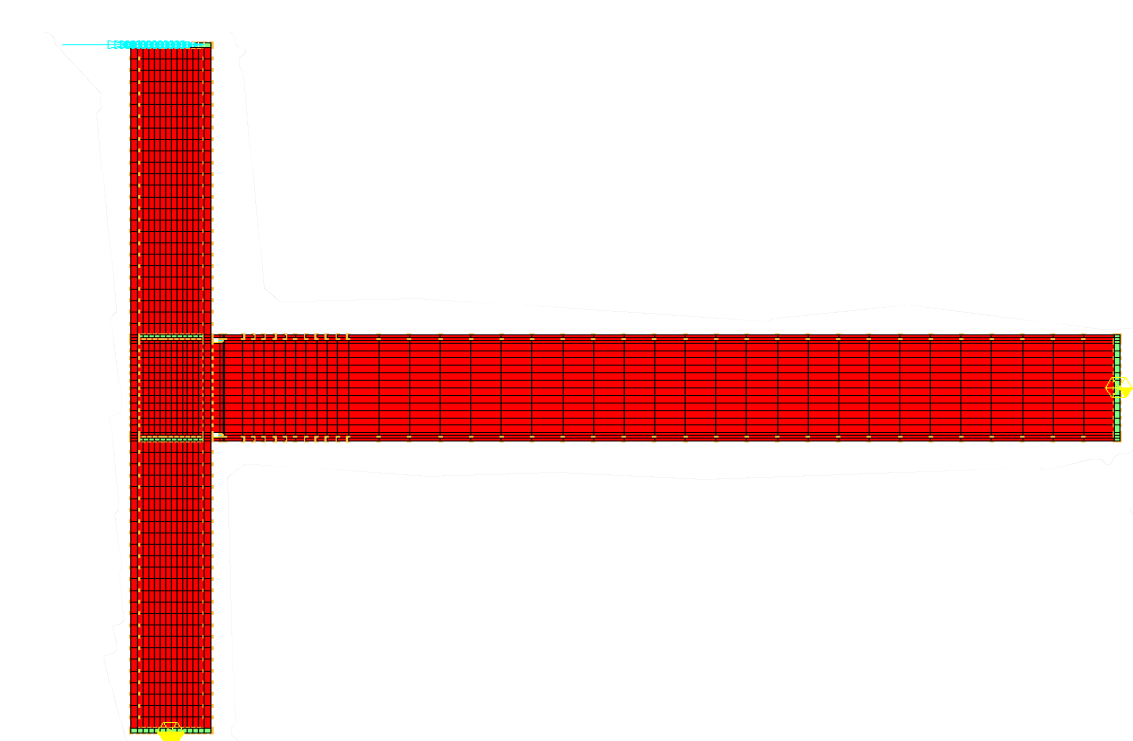


Figure 3.1.4 Typical Model Configuration for Steel Moment Frame using RBS Connection with Loading

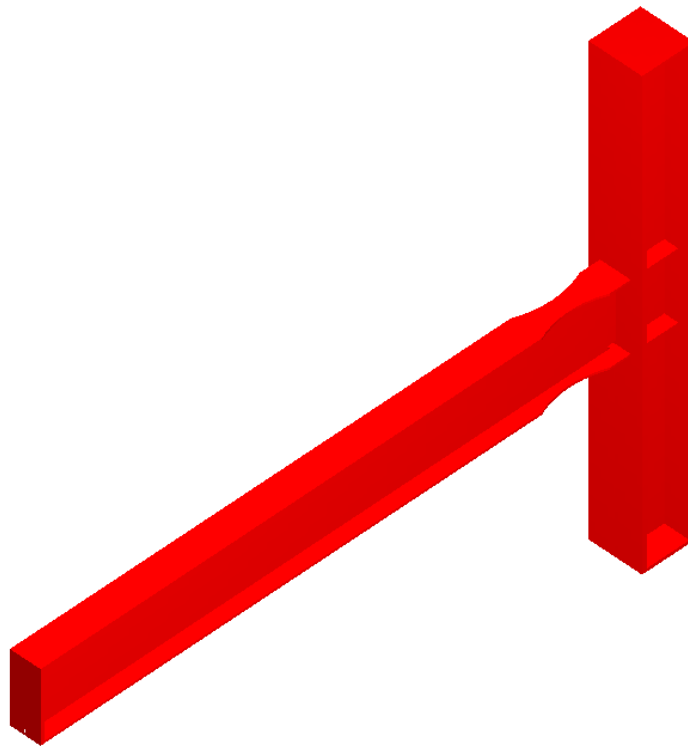


Figure 3.1.5 Isometric View of Typical Model Configuration using RBS Connection

### 3.2 Geometry of the Model

From FEMA 350, section 3.5.5 was followed for designing of Reduced Beam Section Connections. Calculations are shown in detail in the APPENDIX. In this research, two similar types of beam-column connections RBS Straight Cut, and RBS Radius Cut connection were selected for analyzing the connections using Finite Element Software. Model 1 (RBS Straight Cut connection, shown in Figure 3.2.1) and Model 2 (RBS Radius Cut connection, shown in Figure 3.2.2) consist of W24x76 beam and supported by W14x176 column.

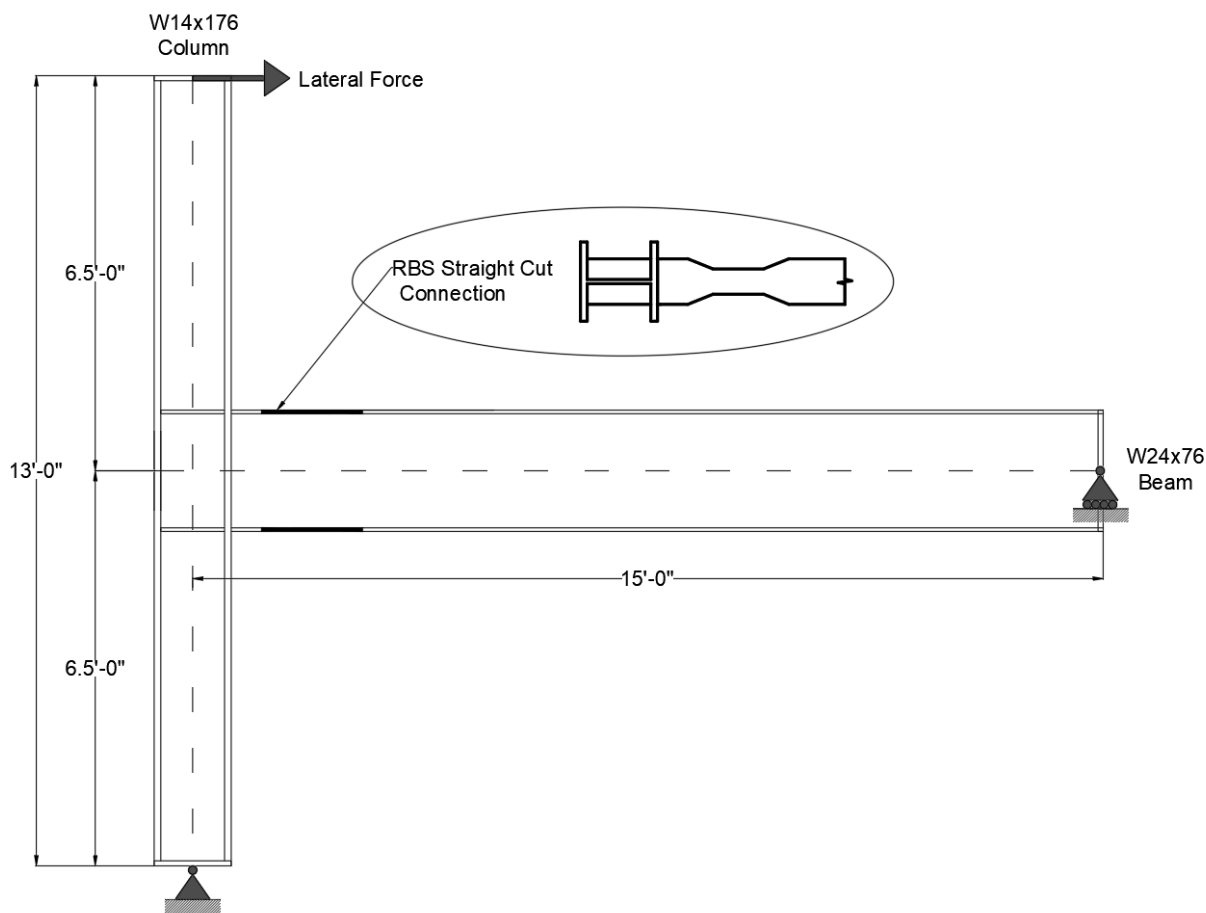


Figure 3.2.1 Model 1, RBS Straight Cut Connection

All the dimensions for the W-Shape column and beams are obtained from Table 1.1 in AISC Steel Construction Manual (AISC 2012).

Both the models in this study require continuity plates and doesn't require doubler plates. It is assumed that the point of inflection occurs at the mid-span of the beam and mid height of the story column. The top of the column is assumed to be free, the roller support is assumed at the end of the beam, and the pinned support is assumed at the base of the column. The lateral loads applied on each model is computed according to the moment capacity values as shown in APPENDIX.

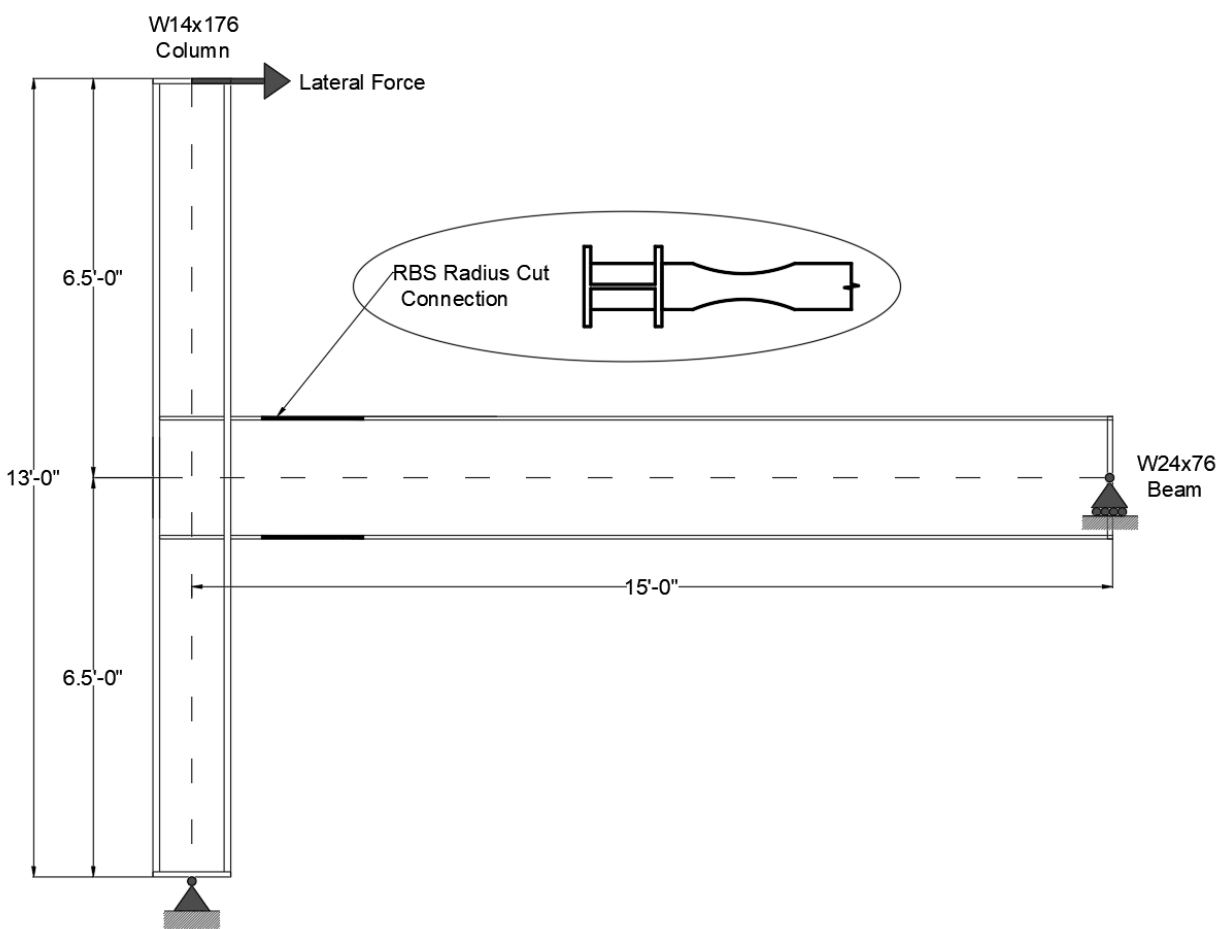


Figure 3.2.2 Model 2, RBS Radius Cut Connection

### 3.3 Material Properties

From the study done by Bartlett (Bartlett et al., 2001), the material used in designing the RBS Connection is A992 Steel. The modulus of elasticity for A992 Steel is used as 29000 ksi and Poisson's Ratio is used as 0.3 for A992 steel. A true stress-strain curve for A992 steel is taken from the study done by Mirza (Mirza, 2014), and it is shown in Figure 3.3.1.

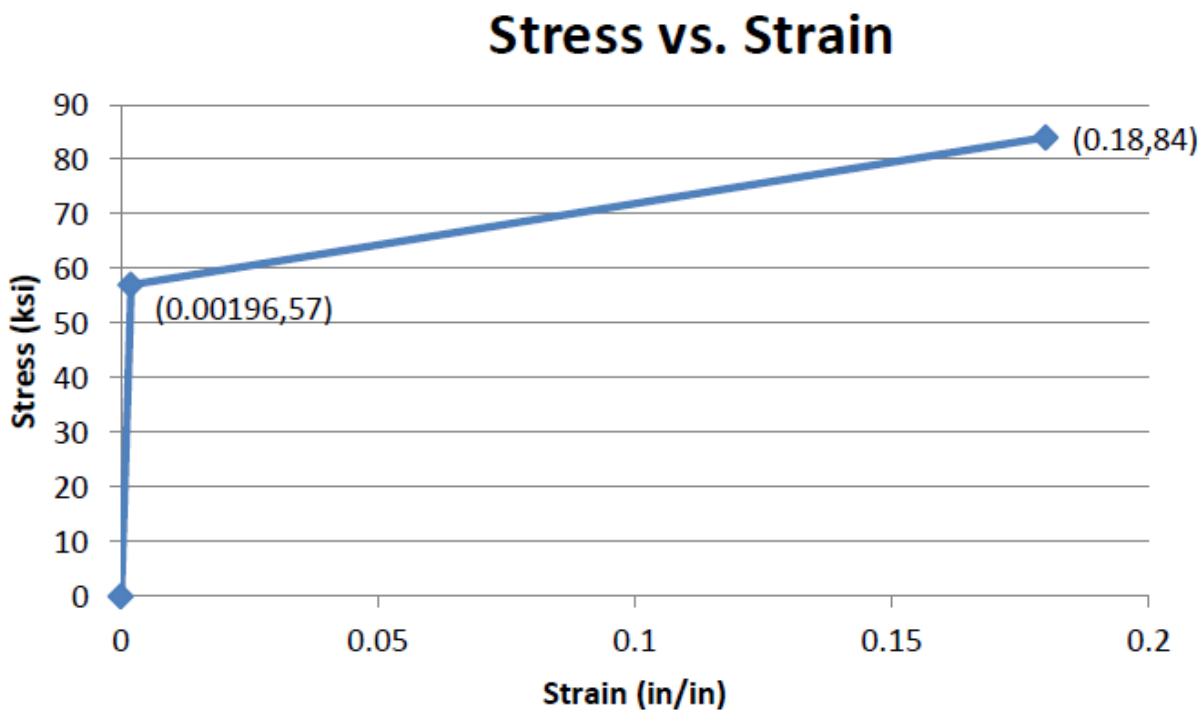


Figure 3.3.1 A True Stress vs. Strain curve for A992 Steel

Table 3.3.1 True Stress vs. Strain Data for A992 Steel

Stress (ksi)	Strain (in/in)
57	0.00196
58	0.002
59	0.01
60	0.017
84	0.18

### 3.4 Loads and Boundary Conditions

After specifying the model geometry and defining the material properties, lateral loads were applied. For both the models, vertical load is considered to be zero, lateral load was computed in APPENDIX and it is applied on the top plate of the column in the form of pressure load. By applying the load in the form of pressure the load gets distributed equally on the column as shown in Figure 3.4.1. The lateral loads were applied on the top of column to 100-time steps for Radius Cut and 500-time steps for Straight Cut. A random load is used for the Finite Element Model analysis of RBS Connection. Here the time steps refer that lateral loads that are applied on the column with the 100 increments the load for Radius Cut and 500 increments the load for Straight Cut in a certain time period to reach the random load. After getting the results, the actual load is computed by multiplying the random load to the respective time step and dividing it by total number of time steps. Then the actual load was compared with the load obtained from the hand calculation, further details are explained in APPENDIX.

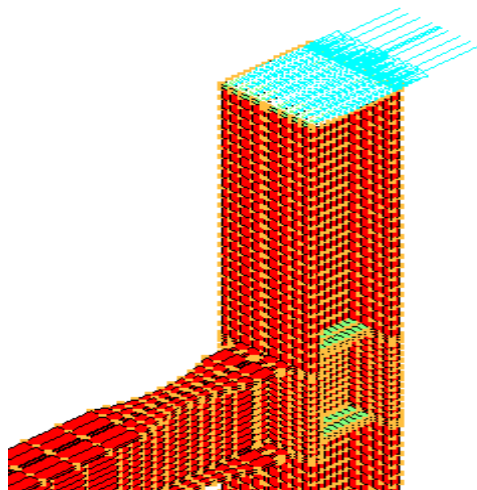


Figure 3.4.1 Typical Distribution of Lateral Load Applied on the Top Plate of the Column

### 3.5 Finite Element Analysis

For both the models, outputs were investigated for first principal stress (84 ksi for A992 steel) and for Von-Mises stress (57 ksi for A992 steel). The first principal stress deals with the fracture in material of the structure. At a certain time step, the A992 steel reaches 84 ksi it means that the elements in the structure have developed fracture and therefore the results after the respective time step at which it reaches 84 ksi are not reliable. At the Von-Mises stress, the structure's material is considered to be yielded or developed plastic hinge at the time step where the model reaches 57 ksi. The time step and also the displacement at the roller support which is located on the end of the beam is recorded, and it is used to compute the stiffness and ductility for both the models.

## CHAPTER 4

### RESULTS AND DISCUSSION

#### 4.1 Brief Introduction

All the results that are obtained from this research were summarized in this chapter, the connections were designed using FEMA 350 and the models are produced and analyzed linearly and nonlinearly using finite element analysis software (NISA 2010). Displacements were observed in the output files of NISA software and it is used to compute the ductility and the stiffness of the models. Lateral load is applied in the form of pressure load on the top of the column and the roller connection was assumed at the midpoint of the beam which restrains the forces along the plane of applied lateral load.

The major trait of this research is the comparison of strengths, ductility ratio and stiffness of between the radius cut and straight cut of Reduced Beam Section (RBS). Special attention should be taken for the formation of the plastic hinges in the RBS of both straight cut and the radius cut because it plays the major role in this research. By observing the Von-Mises stress distribution in the beam it can be determined whether the plastic hinge formation was occurred or not, if the stress exceeds 57 ksi in Von-Mises stress distribution then it is said that yielding of the beam has occurred. Figure 4.1.1 shows the beginning stage of the formation of plastic hinge.

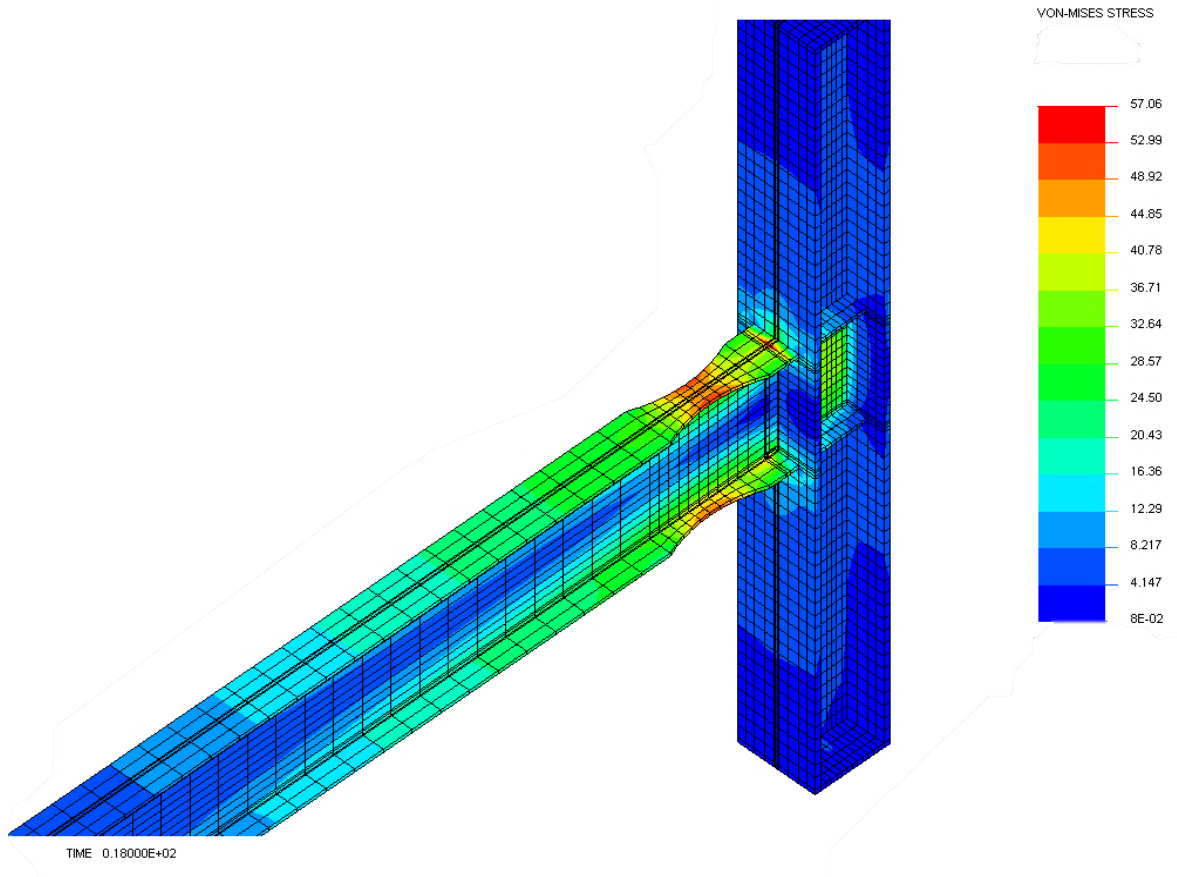


Figure 4.1.1 Beginning of the Formation of Plastic Hinge on RBS

## 4.2 Outputs from Finite Element Analysis Software

One model for reduced beam section – radius cut and another model for reduced beam section – straight cut was analyzed using NISA 2010 and results were obtained. The results were separated into two sections, one section consists of stresses, plastic hinge formation and strength, this section shows that due to the application of lateral loads it causes the yielding and fracture stresses in the models. Another section comprises of lateral displacements and this section is further divided into stiffness and ductility. Each section is briefly described using the pictures obtained from the output files of NISA 2010.

### 4.3 Stresses, Plastic Hinge Formation and Strength

The following section shows the yielding stress, fracture stress, strength and the formation of the plastic hinge achieved for each model from NISA 2010.

#### 4.3.1 Reduced Beam Section – Radius Cut

The radial cut plan view and isometric view of the Reduced Beam Section was shown in figures 4.3.1.1 and 4.3.1.2 respectively.

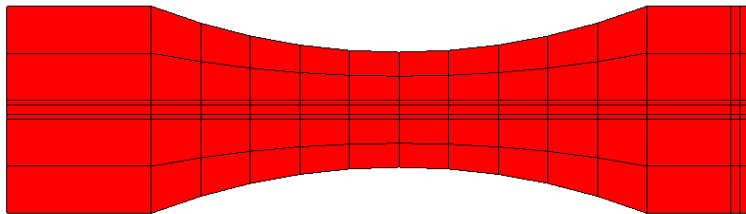


Figure 4.3.1.1 Reduced Beam Section – Radius Cut Plan View

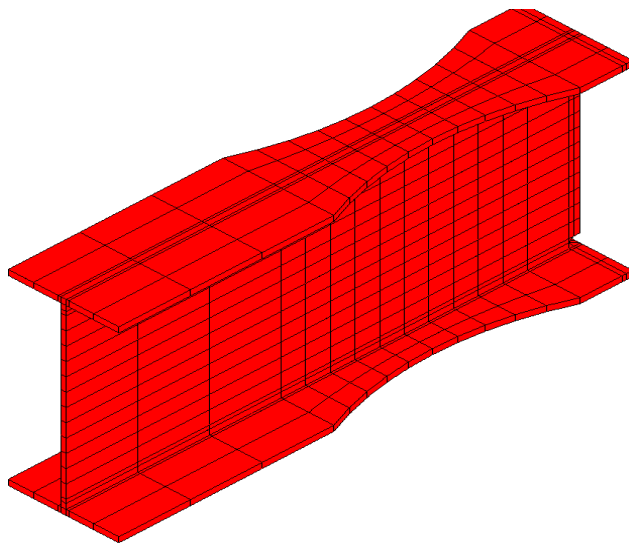


Figure 4.3.1.2 Reduced Beam Section – Radius Cut Isometric View

Figure 4.3.1.3 and Figure 4.3.1.4 shows the 1<sup>st</sup> principal stress and Von-Mises stress for RBS-Radius Cut Model respectively. The 1<sup>st</sup> principal stress reaches 84 ksi at time step 28 and the Von-Mises stress reaches 57 ksi at time step 18. In this model a lateral load of 222 kips was applied in the form of pressure load on the top plate of the column. Lateral load applied at time step 28 when the 1<sup>st</sup> principal stress for the model reaches 84 ksi is 62.16 kips ( $222 \text{ kips} \times \frac{28}{100} = 62.16 \text{ kips}$ ) which is almost near to the to the lateral load obtained in hand calculations (63.85 kips).

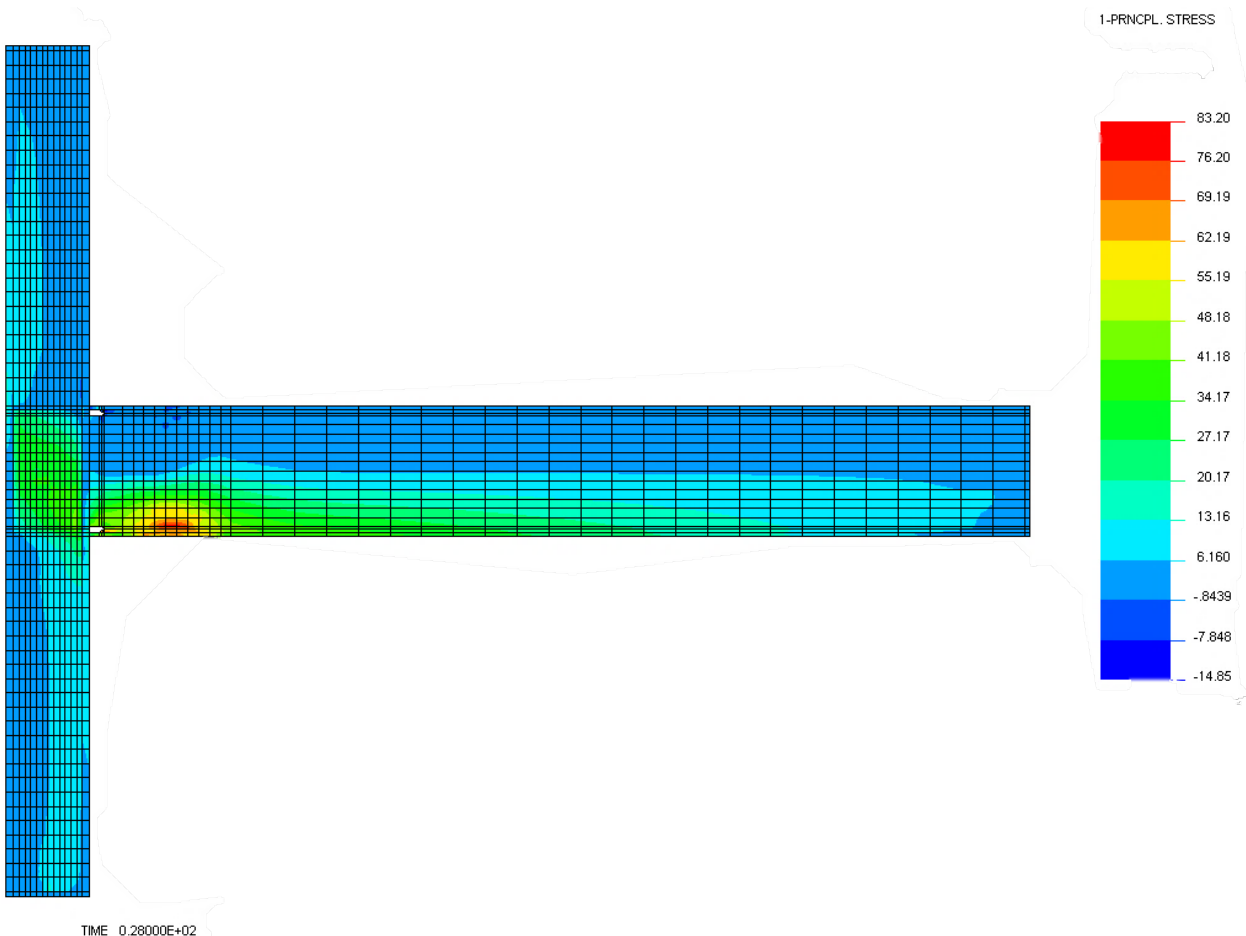


Figure 4.3.1.3 The 1st Principal Stress at 84 ksi (RBS – Radius Cut Model)

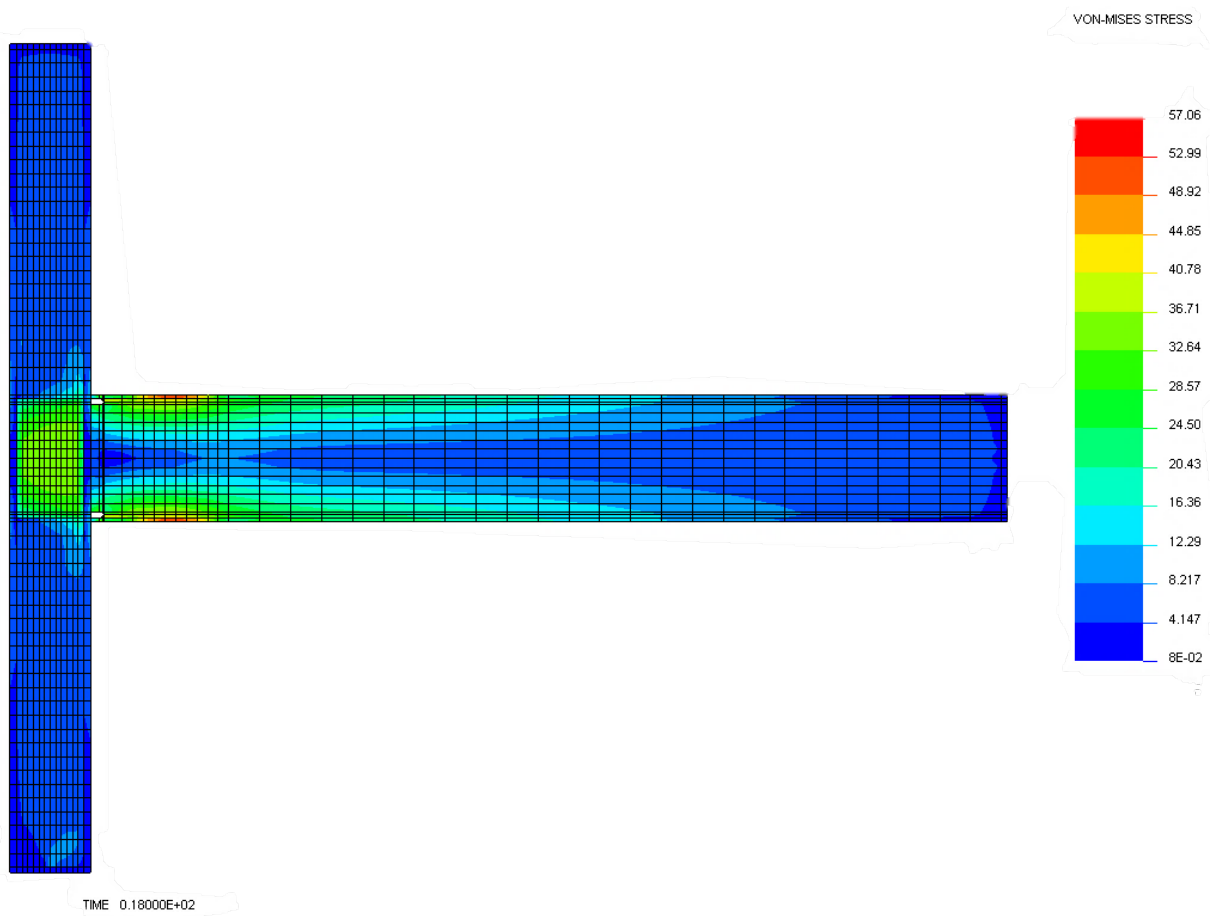


Figure 4.3.1.4 Von-Mises Stress at 57 ksi (RBS – Radius Cut Model)

Figure 4.3.1.5 shows the maximum lateral displacement (2.426 in) of the model at the time step 28 when 1<sup>st</sup> principal stress is equal to 84 ksi. The maximum displacement at this time step can be used to compute the ductility ratio of the model when 1<sup>st</sup> principal stress is at 84 ksi.

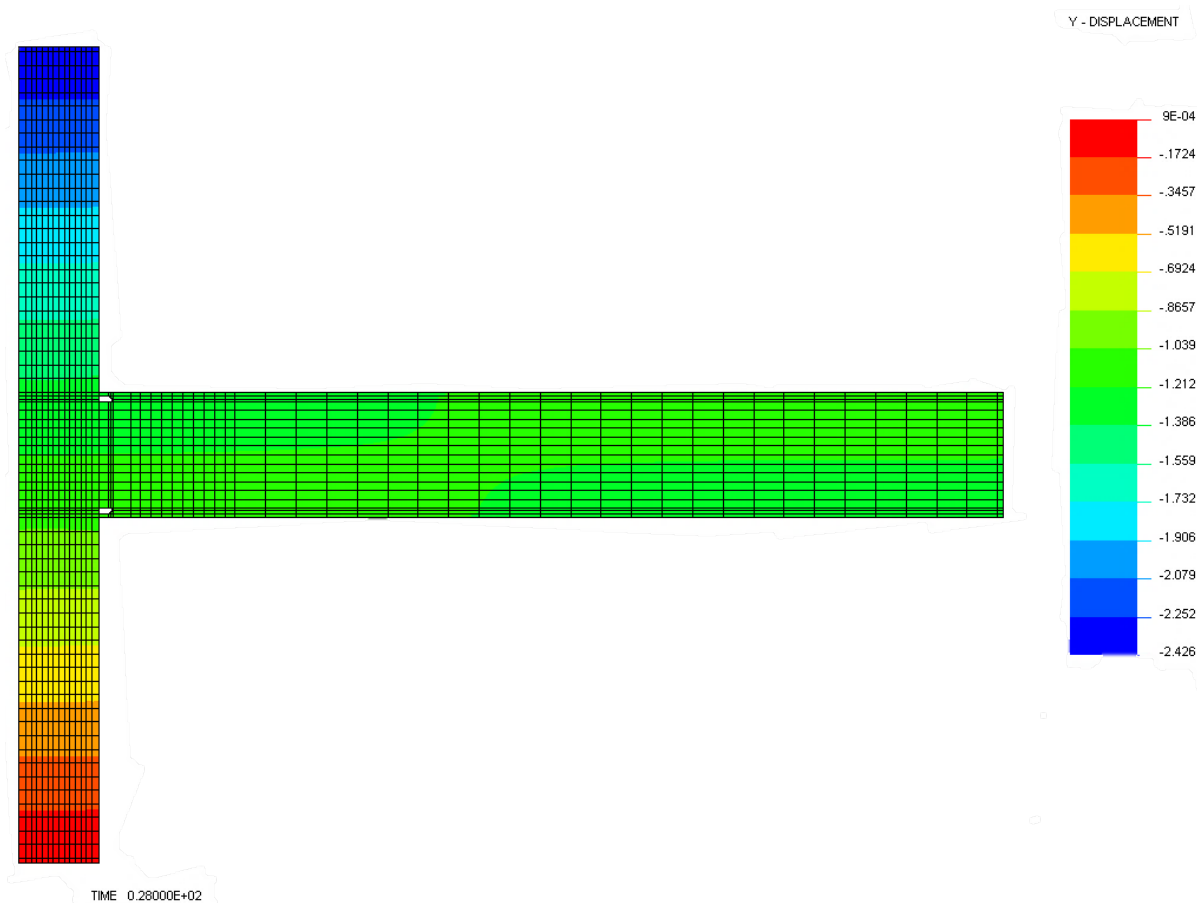


Figure 4.3.1.5 Lateral Displacement when 1<sup>st</sup> Principal Stress is at 84 ksi

(RBS – Radius Cut Model)

Figure 4.3.1.6 represents the maximum lateral displacement (1.405 in) of the model at the time step 18 when Von-Mises stress is equal to 57 ksi. The maximum displacement at this time step can be used to compute the stiffness of the model when Von-Mises stress is at 57 ksi.

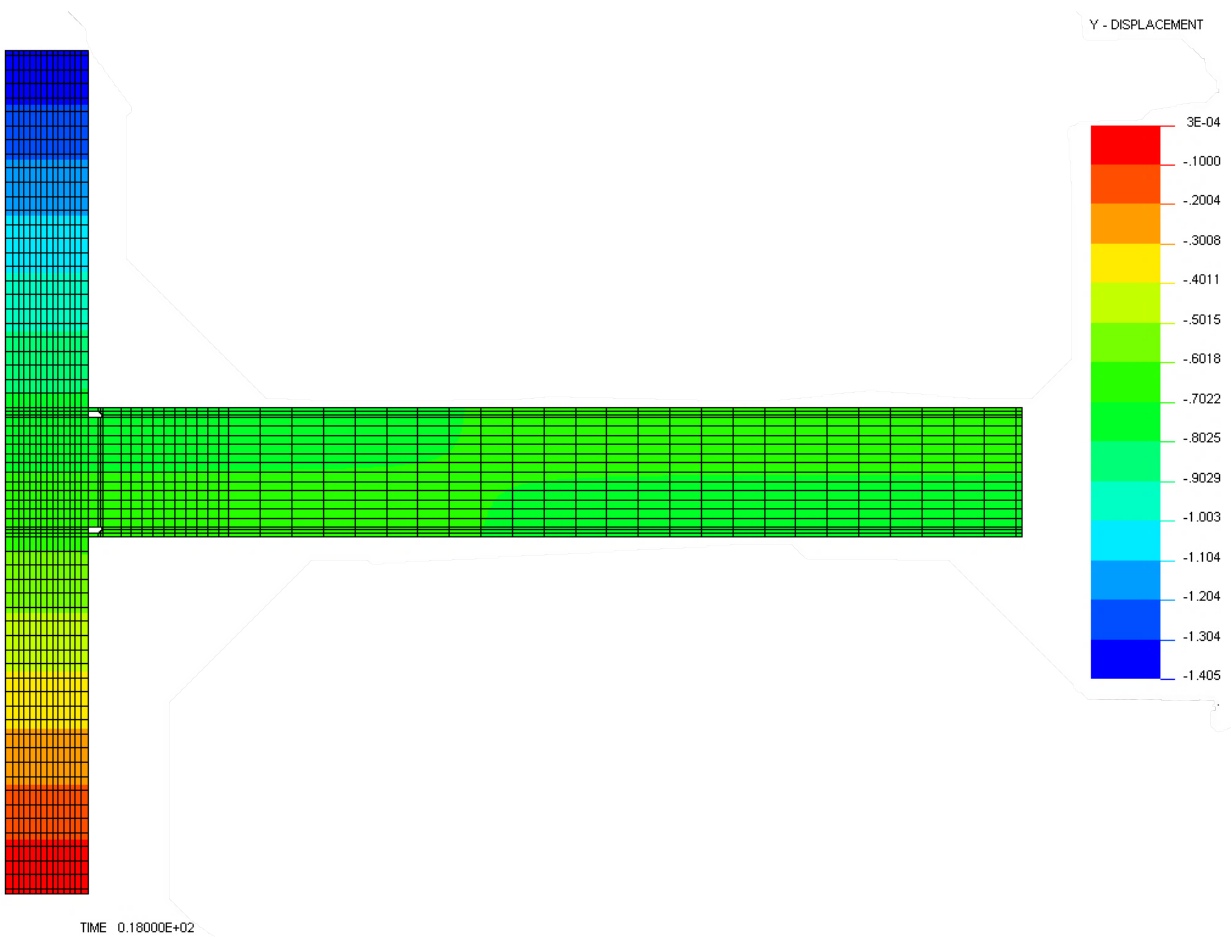


Figure 4.3.1.6 Lateral Displacement when Von-Mises Stress is at 57 ksi  
(RBS – Radius Cut Model)

Figure 4.3.1.7 shows the Von-Mises stress distribution and formation of plastic hinge in RBS- Radius Cut Model. From figure 4.3.1.7 it can be seen that plastic hinges are forming away from the face of the column within the reduced beam area. This proves that one of our objectives for providing reduced beam connection, which is to change the location of the plastic hinge to occur away from the face of the column and it is achieved.

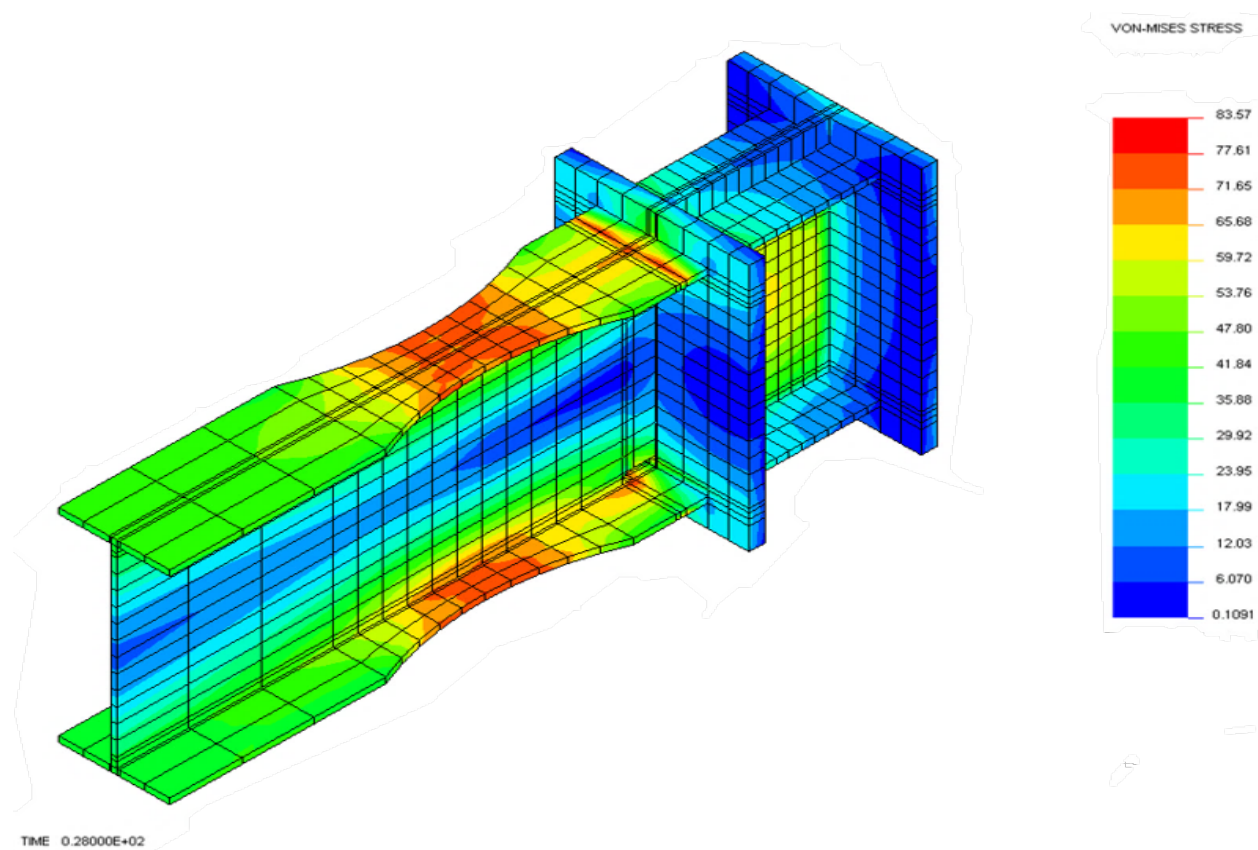


Figure 4.3.1.7 Von-Mises Stress Distribution (RBS – Radius Cut Model)

The Figure 4.3.1.8 represents the Von-Mises stress for the time step-28 same as the time step at which 1<sup>st</sup> principal stress of the model is 84 ksi (time step-28) and this figure shows the location of the final plastic hinge.

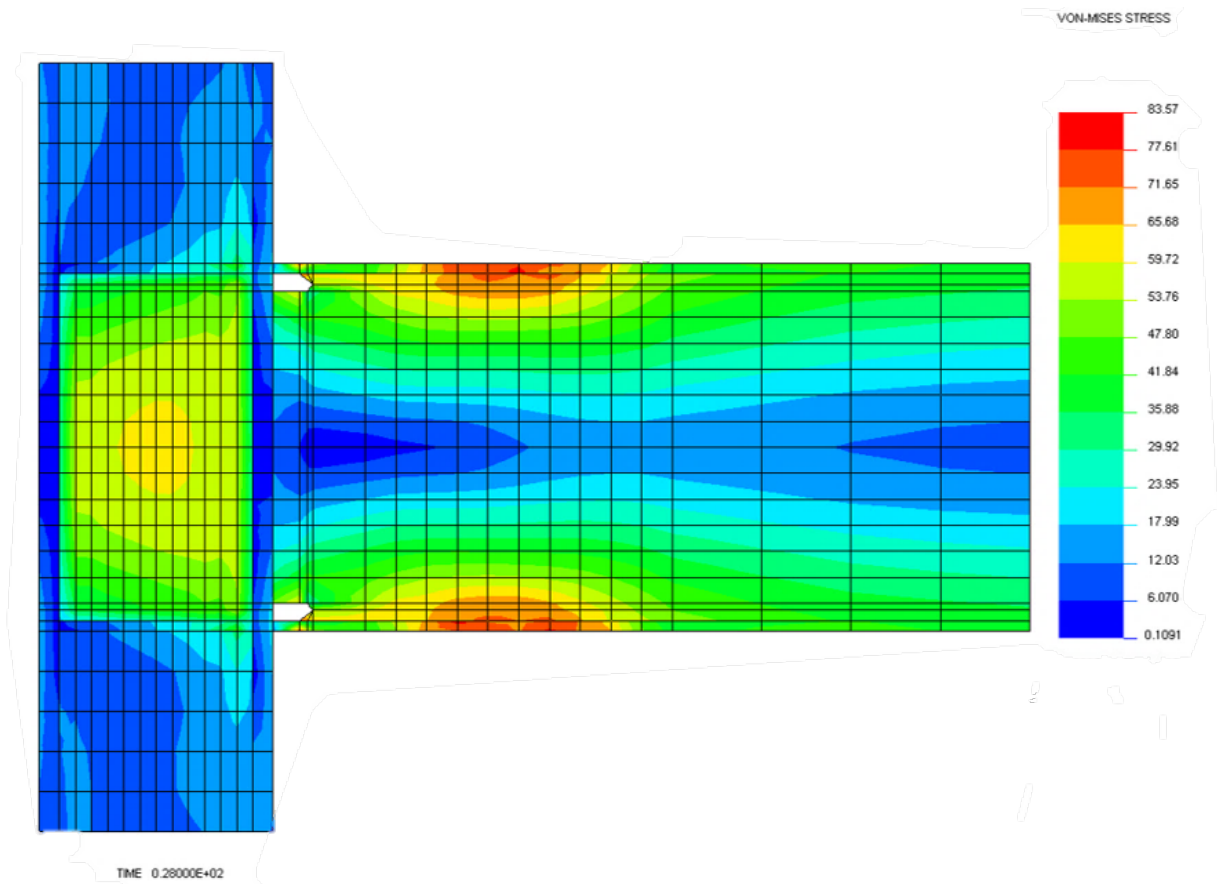


Figure 4.3.1.8 Final Plastic Hinge Formation (RBS – Radius Cut Model)

#### 4.3.2 Reduced Beam Section – Straight Cut

The straight cut plan view and isometric view of the Reduced Beam Section was shown in figures 4.3.2.1 and 4.3.2.2 respectively.

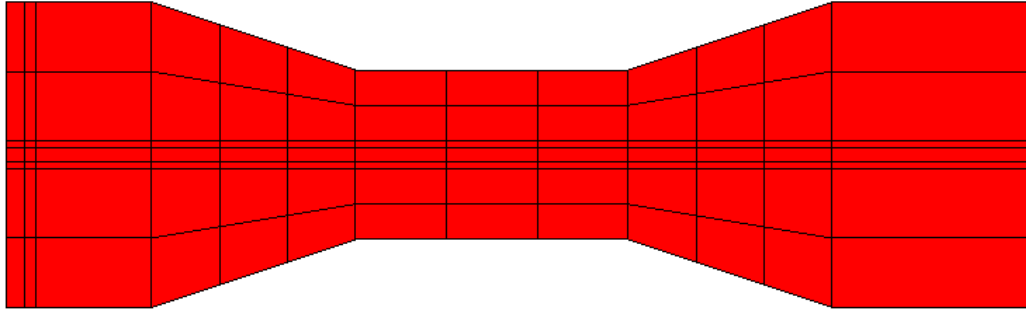


Figure 4.3.2.1 Reduced Beam Section – Straight Cut Plan View

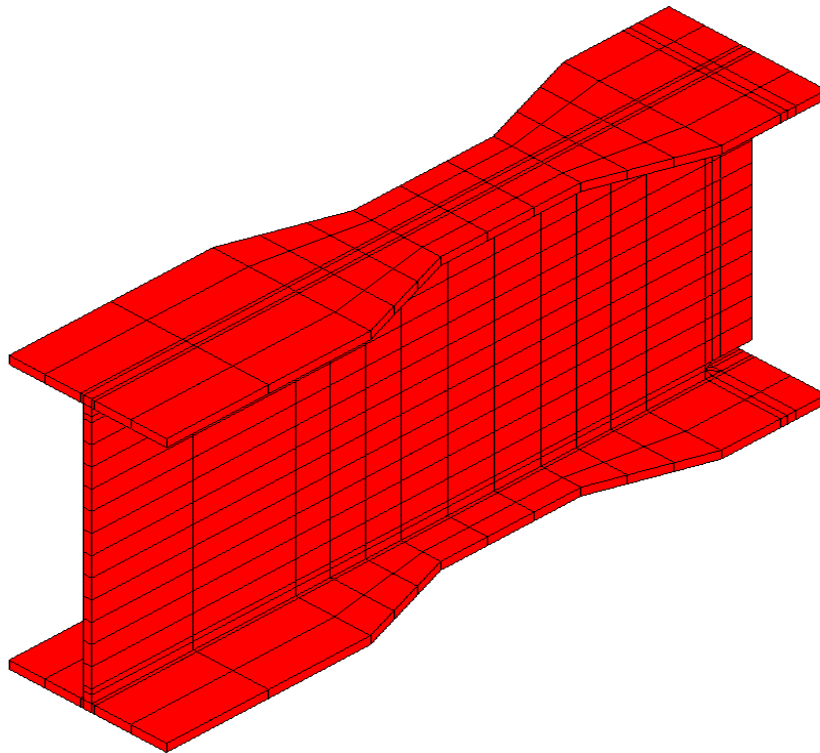


Figure 4.3.2.2 Reduced Beam Section – Straight Cut Isometric View

Figure 4.3.2.3 and Figure 4.3.2.4 shows the 1<sup>st</sup> principal stress and Von-Mises stress for RBS-Straight Cut Model respectively. The 1<sup>st</sup> principal stress reaches 84 ksi at time step 136 (total time step for this model is 500) and the Von-Mises stress reaches 57 ksi at time step 90. In this model a lateral load of 222 kips was applied in the form of pressure load on the top of the column. Lateral load applied at time step 136 when 1<sup>st</sup> principal stress of the model reaches 84 ksi is 60.38 kips ( $222 \text{ kips} \times \frac{136}{500} = 60.38 \text{ kips}$ ) which is almost near to the lateral load obtained in hand calculations (63.85 kips).

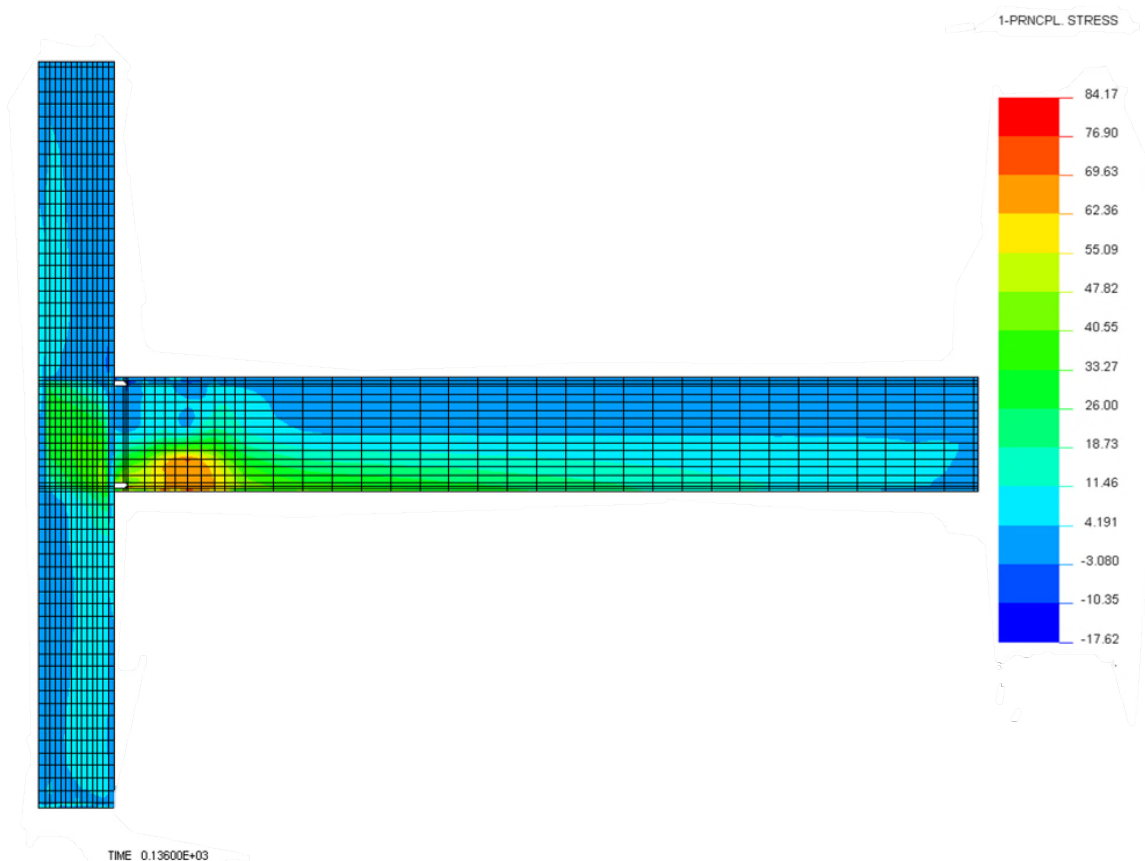


Figure 4.3.2.3 1st Principal Stress at 84 ksi (RBS – Straight Cut Model)

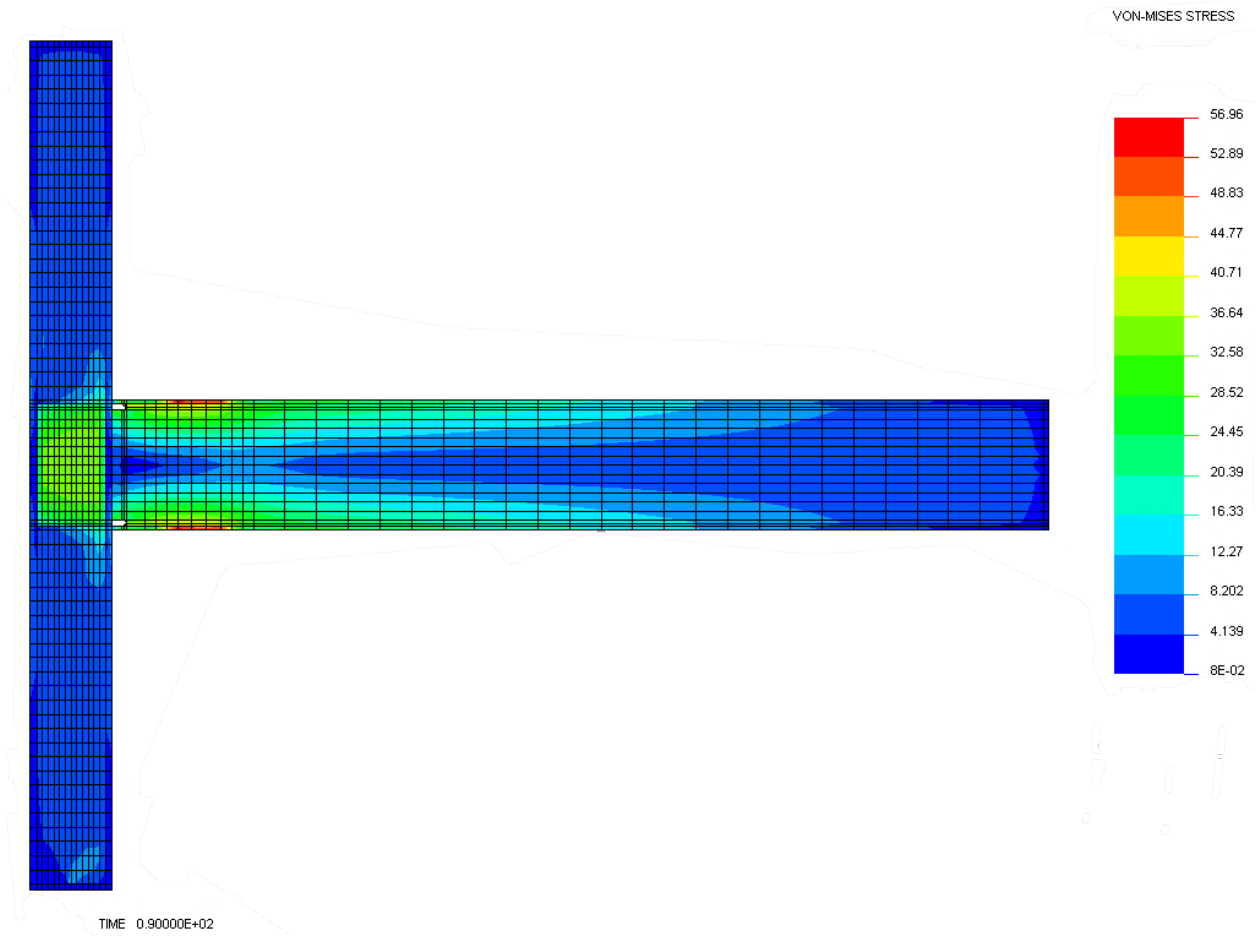


Figure 4.3.2.4 Von-Mises Stress at 57 ksi (RBS – Straight Cut Model)

Figure 4.3.2.5 shows the maximum lateral displacement (2.576 in) of the model at the time step 136 when 1<sup>st</sup> principal stress is equal to 84 ksi. The maximum displacement at this time step can be used to compute the ductility ratio of the model when 1<sup>st</sup> principal stress is at 84 ksi.

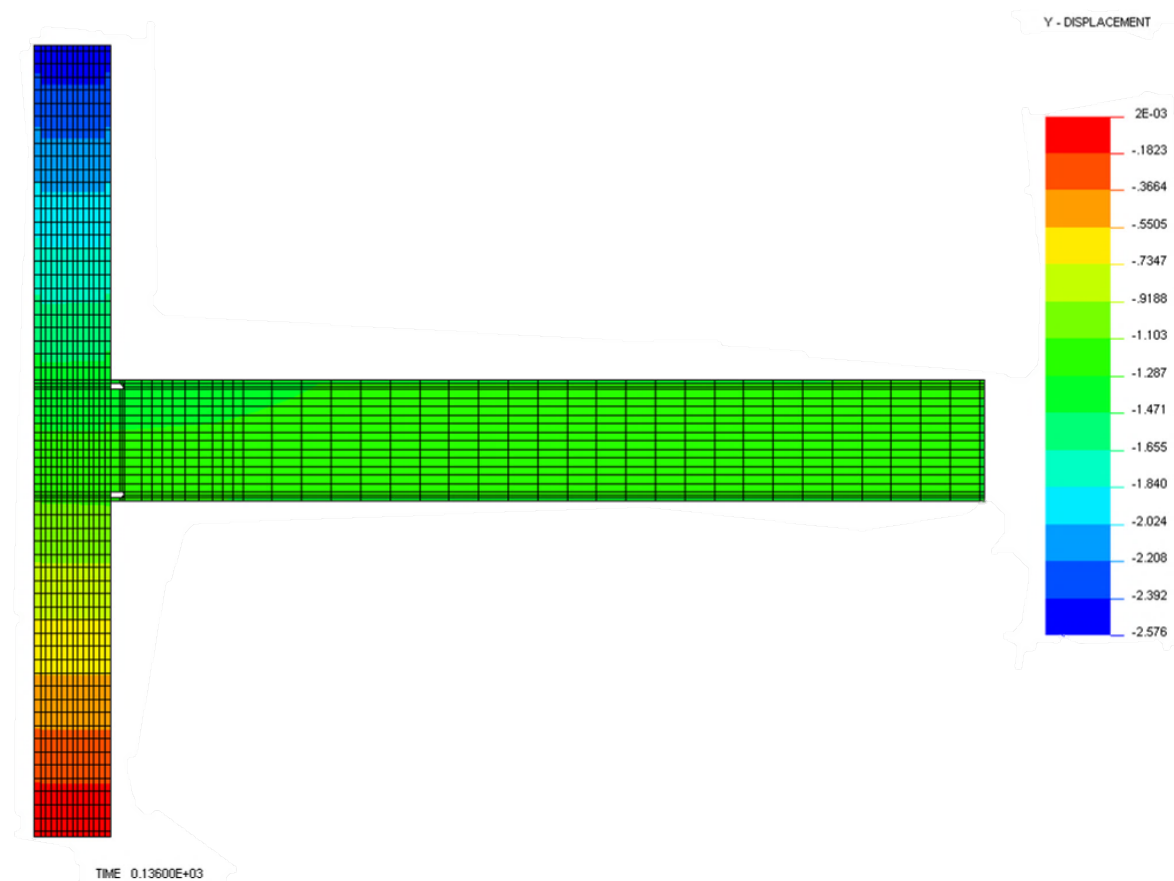


Figure 4.3.2.5 Lateral Displacement when 1<sup>st</sup> Principal Stress is at 84 ksi  
(RBS – Straight Cut Model)

Figure 4.3.2.6 represents the maximum lateral displacement (1.414 in) of the model at the time step 90 when Von-Mises stress is equal to 57 ksi. The maximum displacement at this time step can be used to compute the stiffness and the ductility ratio of the model when Von-Mises stress is at 57 ksi.

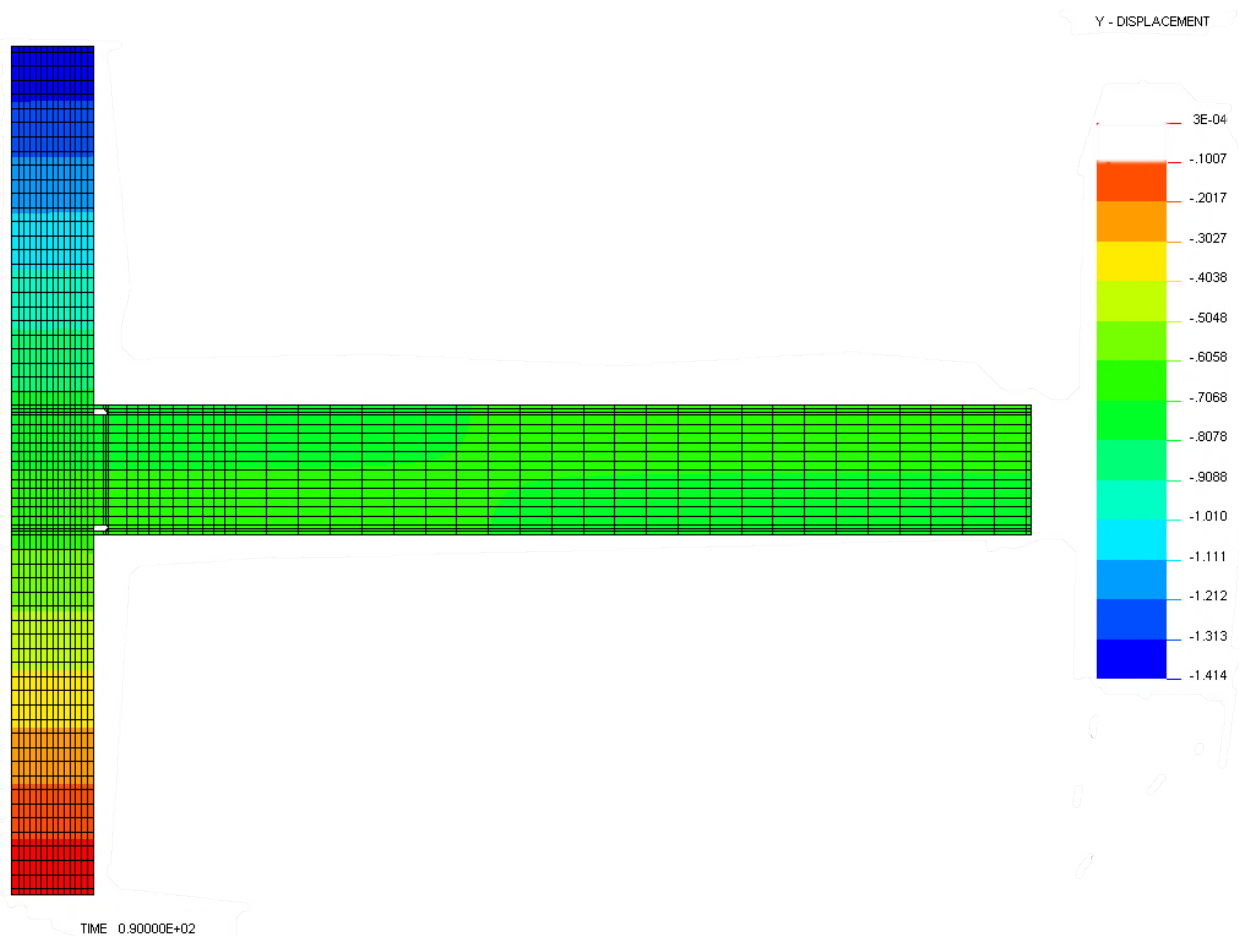


Figure 4.3.2.6 Lateral Displacement when Von-Mises Stress is at 57 ksi  
(RBS – Straight Cut Model)

Figure 4.3.2.7 shows the Von-Mises stress distribution and formation of plastic hinge in RBS- Radius Cut Model. From the Figure 4.3.2.7 it can be seen that plastic hinges are forming away from the face of the column within the reduced beam area. This proves that one of our objectives for providing reduced beam connection, which is to change the location of the plastic hinge to occur away from the face of the column and it is achieved.

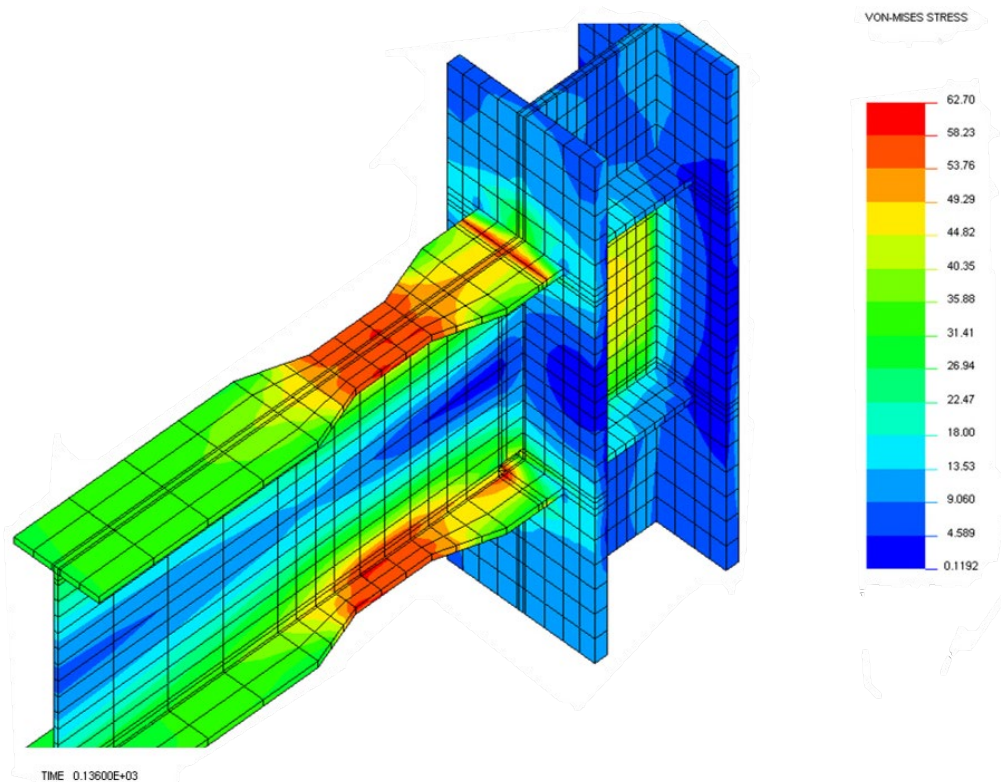


Figure 4.3.2.7 Von-Mises Stress Distribution (RBS – Straight Cut Model)

Figure 4.3.2.8 represents the Von-Mises stress for the time step-136 same as the time step at which 1<sup>st</sup> principal stress of the model is close to 84 ksi (time step-136) and this figure shows the location of the final plastic hinge.

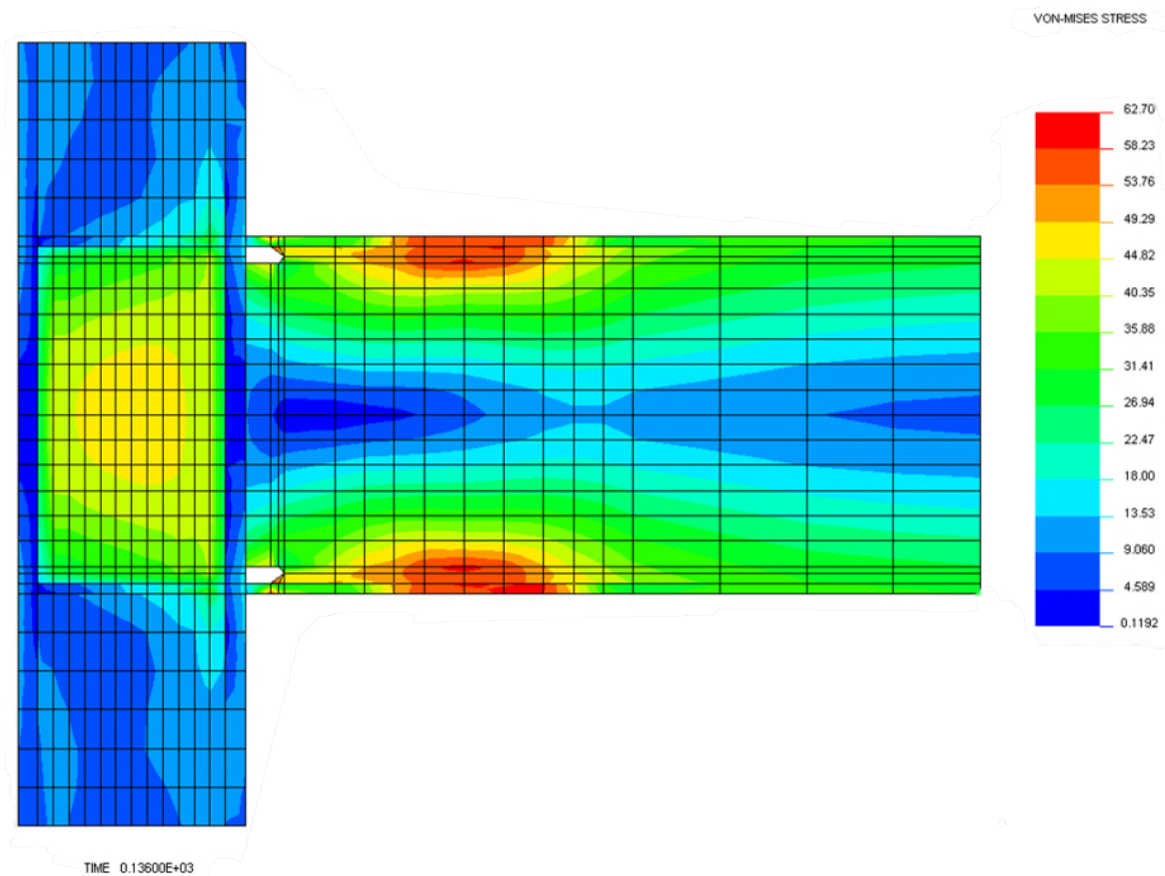


Figure 4.3.2.8 Final Plastic Hinge Formation (RBS – Straight Cut Model)

#### 4.4 Lateral Load Applied on the Models

Lateral load is calculated for all the models when 1<sup>st</sup> principal stress reaches 84 ksi and when Von-Mises stress reaches 57 ksi.

#### 4.4.1 Lateral Load when 1<sup>st</sup> Principal Stress is at 84 ksi

Table 4.4.1 shows the calculations of lateral loads for RBS-radius cut and RBS-straight cut. A lateral load of 222 kips is applied on both the models, when the 1<sup>st</sup> principal stress reaches 84 ksi, lateral load applied at that time step is calculated and cross checked with the lateral load obtained from the hand calculations.

Table 4.4.1.1 Lateral Load Calculations When 1<sup>st</sup> Principal Stress Reaches 84 ksi

RBS Models	Time Steps	Total Time steps	Lateral load (kips) when 1st Principal Stress is 84 ksi	Lateral Load (Kips) from Hand Calculations
Radius Cut	28	100	$\frac{28 \times 222}{100} = 62.16$	63.85
Straight Cut	136	500	$\frac{136 \times 222}{500} = 60.38$	63.85

#### 4.4.2 Lateral Load when Von-Mises Stress Reaches at 57 ksi

Table 4.4.2.1 shows the calculations of lateral loads for RBS-radius cut and RBS-straight cut. A lateral load of 222 kips is applied on both the models, when the Von-Mises stress reaches 57 ksi, lateral load applied at that time step is calculated and it is used to determine the stiffness of the models.

Table 4.4.2.1 Lateral Load Calculations when Von-Mises Stress Reaches 57 ksi

RBS Models	Time Steps	Total Time Steps	Lateral Load (kips) when Von-Mises Reaches 57 ksi
Radius Cut	18	100	$\frac{18 \times 222}{100} = 39.96$
Straight Cut	90	500	$\frac{90 \times 222}{500} = 39.96$

#### 4.5 Displacement and Ductility

Ductility of the reduced beam section can be computed by using the maximum displacements from Figure 4.3.1.5 and Figure 4.3.2.5 when the 1<sup>st</sup> principal stress for model reaches 84 ksi and from the Figure 4.3.1.6 and Figure 4.3.2.6 when the Von-Mises stress reaches 57 ksi.

#### 4.5.1 Lateral Displacement when 1<sup>st</sup> Principal Stress Reaches at 84 ksi

Table 4.5.1.1 shows the displacement for RBS-radius cut and RBS- straight cut models when the 1<sup>st</sup> principal stress reaches 84 ksi. Displacements are recorded at time step-28 for RBS-radius cut and at time step-136 for RBS-straight cut.

Table 4.5.1.1 Lateral Displacements when 1<sup>st</sup> Principal Stress Reaches 84 ksi

RBS Models	Time Steps	Lateral Displacement (in) when 1 <sup>st</sup> Principal Stress is 84 ksi
Radius Cut	28	2.426
Straight Cut	136	2.576

#### 4.5.2 Lateral Displacement when Von-Mises Stress is at 57 ksi

Table 4.5.2.1 shows the displacement for RBS-radius cut and RBS- straight cut models when the Von-Mises stress reaches 57 ksi. Displacements are recorded at time step-18 for RBS-radius cut and at time step-90 for RBS-straight cut.

Table 4.5.2.1 Lateral Displacements when Von-Mises Stress Reaches 57 ksi

RBS Models	Time Steps	Lateral Displacement (in) when Von-Mises Stress is 57 ksi
Radius Cut	18	1.405
Straight Cut	90	1.414

### 4.5.3 Computations and Comparison of Ductility

The lateral displacements shown in Table 4.5.1.1 and in Table 4.5.2.1 are used to compute the ductility for both the models. Ductility is obtained in terms of ratio and it is calculated by dividing the lateral displacement at time step where 1<sup>st</sup> principal stress is 84 ksi to the lateral displacement at the time step where Von-Mises stress reaches 57 ksi. Table 4.5.3.1 gives the calculations performed to obtain ductility ratio for each model and the comparison for the ductility ratio reaches shown in table 4.5.3.2

Table 4.5.3.1 Calculations for Ductility Ratio

RBS Models	Lateral Displacement (in) when 1st principal Stress is 84 ksi	Lateral Displacement (in) when Von-Mises Stress is 57 ksi	Ductility Ratio
Radius Cut	2.426	1.405	$(2.426 / 1.405)$ = 1.73
Straight Cut	2.576	1.414	$(2.576 / 1.414)$ = 1.82

Table 4.5.3.2 Comparison of Ductility Ratio

RBS Models	Lateral Load (ksi)	Lateral Displacement (in) when 1st Principal Stress is 84 ksi	Lateral Displacement (in) when Von-Mises Stress is 57 ksi	Ductility Ratio
Radius Cut	63.85	2.426	1.405	1.73
Straight Cut	60.384	2.576	1.414	1.82

#### 4.6 Stiffness

Stiffness is calculated in the elastic range for both of the models. Time step at which the Von-Mises stress reaches 57 ksi and for the same lateral load record the displacements and it can be used to calculate the stiffness. Table 4.6.1 summarizes the results i.e. Lateral displacement, lateral load of all the models obtained in the elastic range.

Table 4.6.1 Lateral Displacement and Lateral Load when Von-Mises Stress Reaches 57 ksi

RBS Models	Lateral Load (kips) Elastic Range	Lateral Displacement (in)
Radius Cut	39.96	1.405
Straight Cut	39.96	1.414

#### 4.6.1 Computation and Comparison of Stiffness

Stiffness will vary depending on the moment of inertia. In Figure 4.6.1.1, it shows the overlap of straight cut and radius cut. This figure proves that average of the moment of inertia of the cross section throughout the flange  $b$  is more to the RBS Radius Cut than RBS Straight Cut, which means theoretically RBS-Radius Cut should be stiffer than RBS-Straight Cut.

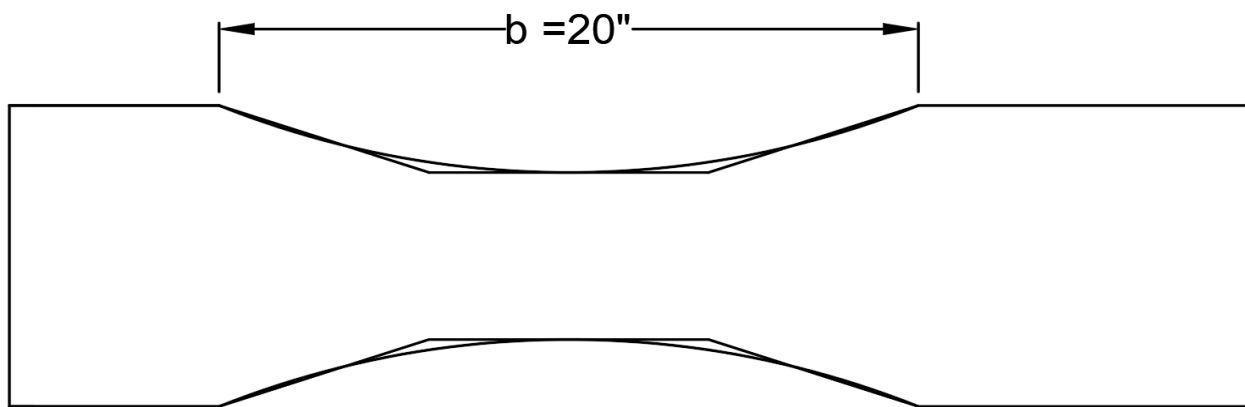


Figure 4.6.1.1 Overlap of RBS – Straight Cut and Radius Cut

Stiffness for each model is calculated by dividing the applied lateral load to the lateral displacement. Table 4.6.1.1 shows the calculations performed to obtain the stiffness for each model within elastic range.

The output from finite element analysis shows that, under the application of same lateral load within the elastic range, RBS-Radius Cut has displaced less as compared to the RBS-Straight Cut connection system. Results from this research indicates that RBS-Radius Cut is stiffer than RBS-Straight Cut

Table 4.6.1.1 Stiffness Computations and Comparison (Elastic Range)

RBS Models	Lateral Load (kips) Elastic Range	Lateral Displacement (in)	Stiffness (k/in)
Radius Cut	39.96	1.405	$(39.96/1.405) =$ 28.44
Straight Cut	39.96	1.414	$(39.96/1.414) =$ 28.26

CHAPTER 5  
SUMMARY AND COMPARISON OF RESULTS

All the results obtained from Finite Element Analysis software (NISA 2010) are summarized and compared in this chapter. Ductility and stiffness were calculated only based on the results obtained from NISA 2010. However, strength in terms of lateral load is calculated by hand calculations and it is also compared with the results from NISA 2010. In Table 5.1 show the summary and comparison of results obtained for each model from NISA 2010 and Table 5.2 compares the strengths for each model obtained from NISA 2010 with hand calculations.

Table 5.1 Comparison and Summary of Results Recorded from the Outputs of NISA 2010

Model	RBS - Radius Cut	RBS - Straight Cut
Beam Section	W24x76	W24x76
Column Section	W14x176	W14x176
Ultimate Strength (kips) (In terms of Lateral Capacity)	62.16	60.384
Yield Strength (kips)	39.96	39.96
Ductility (ratio)	1.73	1.82
Stiffness (kips/in) Elastic Range	28.44	28.26

Table 5.2 Comparison of Strengths Obtained from Finite Element Analysis and Hand Calculations

Model	RBS - Radius Cut	RBS – Straight Cut
Beam Section	W24x76	W24x76
Column Section	W14x176	W14x176
Ultimate Strength from Finite Element Analysis (kips)	62.16	60.38
Ultimate Strength from Hand Calculations (kips)	63.85	63.85
% Error of Ultimate Strength from hand calculations and Finite Element Results	2.64%	5.44%

## CHAPTER 6

### CONCLUSION

It is impossible to make structures invulnerable to sustain the forces from earthquake. The basic idea of design technique is to provide structures with an ability to sustain immense ground shaking without collapse but with a reasonable structural damage. The objective of design is to construct a structure which can withstand huge amount of inelastic deformation without fracture at the connection.

The purpose of this research is to study the comparison of strength, ductility, and stiffness of the two different types of Reduced Beam Section connections i.e. straight cut and radius cut. Finite element analysis software is used to model and analyze the connections. From the results of finite element analysis, 1<sup>st</sup> Principal Stress, Von-Mises Stress, applied lateral loads, lateral displacements were observed, and comparison was made between two models based on their ductility, stiffness and strength.

Ductility is calculated by dividing the lateral displacement of the frame with RBS connection at fracture to the lateral displacement of the frame with RBS connection at yield. The results from the finite element analysis says that RBS – Straight Cut connection is more ductile than RBS – Radius Cut connection.

In terms of strength, the lateral load obtained from hand calculations for both the models is same. However, the results from finite element analysis indicates that RBS-Radius Cut is able to hold more lateral load as compared to RBS-Straight cut connection. This is because the average of the  $I$  (moment of inertia) value within the RBS-Radius Cut is higher than RBS-Straight Cut.

Stiffness was also computed for both connections from finite element analysis. Generally, RBS-Radius Cut is stiffer than RBS-Straight Cut. This is because the average of the  $I$  (moment of inertia) value within the RBS-Radius Cut is higher than RBS-Straight Cut.

Based on the examples used in this study the results conclude that, Reduced Beam Section - Radius cut has more or higher strength, more stiffness but less ductile as compared to Reduced Beam Section - Straight Cut.

## REFERENCES

- American Institute of Steel Construction (AISC). (2012). *Manual of Steel Construction. 15th Ed.*, Chicago, IL.
- American Institute of Steel Construction (AISC). (2016). *Seismic Provisions for Structural Steel Buildings. 3rd Ed.*, Chicago, IL.
- Bartlett, F. M., Dexter, R. J., Graeser, M. D., Jelinek, J. J., Schmidt, B. J., & Galambos, T. V. (2001). *Updating standard shape material properties database for design and reliability (K-Area 4)*. Technical Report for American Institute of Steel Construction.
- Chen, S. J., Yeh, C. H., & Chu, J. M. (1996). Ductile steel beam-to-column connections for seismic resistance. *Journal of Structural Engineering*, 122(11), 1292-1299.
- FEMA-350, (2000). *Recommended Seismic Design Criteria for New Moment-Resisting Steel Frame Structures*, prepared by the SAC Joint Venture for the Federal Emergency Management Agency, Washington.
- Hamburger, R. O., Hamburger, R. O., & Malley, J. O. (2009). *Seismic design of steel special moment frames: a guide for practicing engineers*. National Earthquake Hazards Reduction Program.
- Hernandez, A. (2016). "Plastic hinge location effects on the design of welded flange plate connections." (Master's Thesis), Southern Illinois University at Carbondale.
- Hwang, S. H., Choi, B. G., Moon, K. H., & Han, S. W. (2009). New Procedure for Estimating the Moment Strength of Reduced Beam Section Connections with Bolted Webs. In *The 5th International Symposium on Steel Structures, Seoul, Korea*.
- Mao, C., Ricles, J., Lu, L. W., & Fisher, J. (2001). Effect of local details on ductility of welded moment connections. *Journal of Structural engineering*, 127(9), 1036-1044.
- McEntee, P. (2009). "Steel moment Frames-History and Evolution." *Structural Engineering Magazine, Simpson Strong-Tie*, 1-6.
- Mirza, M. B. (2014). Comparison of Strength, Ductility and Stiffness of Reduced Beam Section and Welded Flange Plate Connection.
- NISA/DISPLAY IV Ver.17.0 (Finite Element Software). (2010). Engineering Mechanics Research Corporation Troy, MI

- Plumier, A. (1997). "The dogbone: Back to the future." *Engineering Journal*, ASIC, 34(2), 61–67.
- Popov, E. P., Yang, T. S., & Chang, S. P. (1998). Design of steel MRF connections before and after 1994 Northridge earthquake<sup>1</sup>. *Engineering Structures*, 20(12), 1030-1038
- Roeder, C. W. (2002). Connection performance for seismic design of steel moment frames. *Journal of Structural Engineering*, 128(4), 517-525.
- Shi, Y., Wang, M., & Wang, Y. (2012). Analysis of Seismic Behavior of Welded Steel Connections and Frames with Differently Constructed Connections. *Advances in Structural Engineering*, 15(7), 1053-1068.
- Tremblay, R., Filiatrault, A., Timler, P., & Bruneau, M. (1995). Performance of steel structures during the 1994 Northridge earthquake. *Canadian Journal of Civil Engineering*, 22(2), 338-360.
- Tsavaridis, K. D. (2014). Strengthening techniques: code-deficient steel buildings. In *Encyclopedia of earthquake engineering* (pp. 1-26). Springer, Berlin, Heidelberg.

## APPENDICES

## APPENDIX A

## DESIGN PROCEDURE

Design calculations for Reduced Beam Section Connection (Beam W24x76, Column W14x176)

In reference to 'Recommended Seismic Design Criteria for New Steel Moment – Frame Buildings (FEMA-350, 2000)

Table A.1 Section Properties for the Beam and Column for both Models

	Section	d (in)	$b_f$ (in)	$t_w$ (in)	$t_f$ (in)	$S_x$ (in <sup>3</sup> )	$Z_x$ (in <sup>3</sup> )	L/2 (ft)
Beam	W24x76	23.9	8.99	0.44	0.68	176	200	15
Column	W14x176	15.2	15.7	0.83	1.31	281	320	6.5

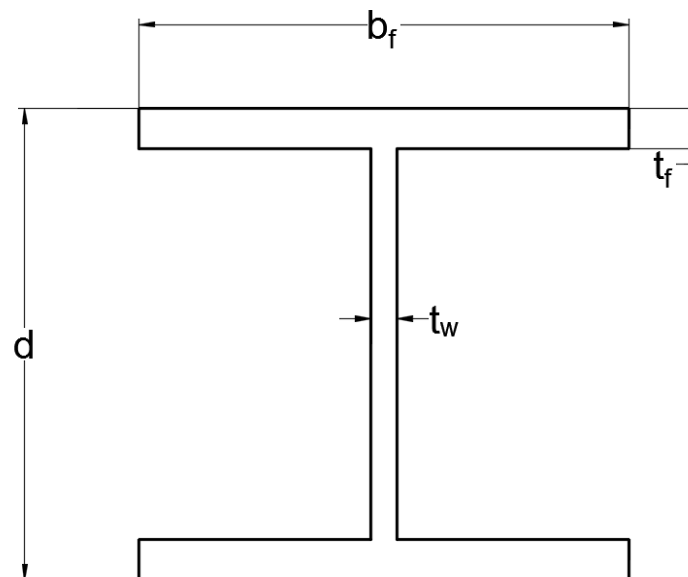


Figure A1: Dimensions of a W section

### 3.5.5.1 Design Procedure:

Step 1: Determine the length and location of the beam flange reduction, based on the following:

$$\begin{aligned}
 a &= (0.5 \text{ to } 0.75) b_f \\
 &= (0.5b_f) \text{ to } (0.75b_f) \\
 &= (0.5) (8.99) \text{ to } (0.75) (8.99) \\
 &= 4.5 \text{ in to } 6.74 \text{ in}
 \end{aligned}$$

Choose  $a = 6 \text{ in}$

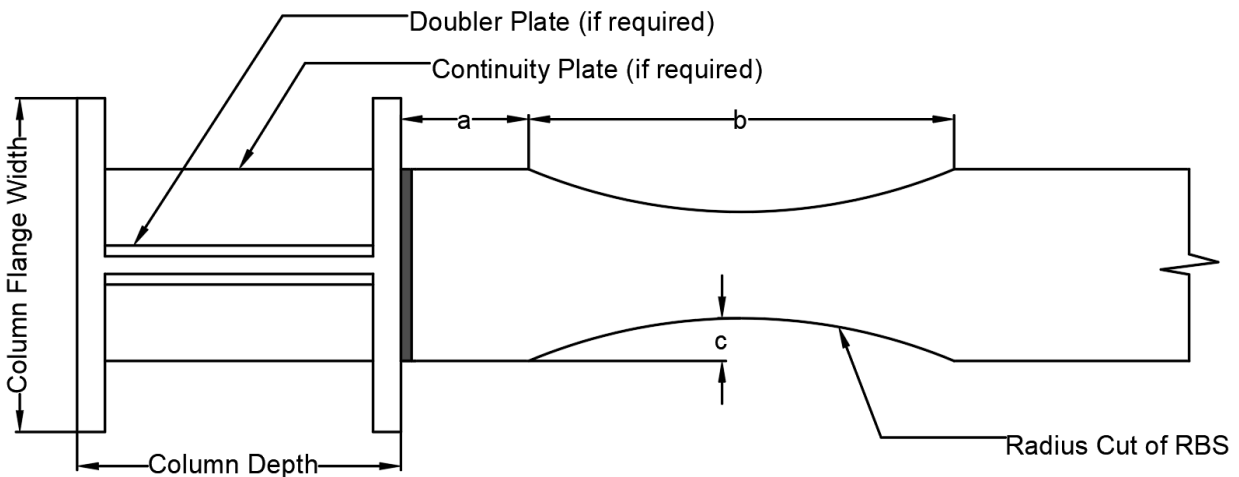


Figure A2: Reduced Beam Section Connection (Radius Cut)

$$\begin{aligned}
 b &= (0.65 \text{ to } 0.85) (d_b) \\
 &= (0.65 d_b) \text{ to } (0.85d_b) \\
 &= (0.65)(23.9) \text{ to } (0.85)(23.9) \\
 &= 15.53 \text{ in to } 20.32 \text{ in} \\
 &\text{Choose } b = 20 \text{ in}
 \end{aligned}$$

Step 2: Determine the depth of the flange reduction,  $c$ , according to the following:

$$\begin{aligned}
 \text{a) Assume } c &= 0.20b_f \\
 c &= (0.2)b_f \\
 c &= (0.2)(8.99) \text{ in} \\
 c &= 1.8 \text{ in}
 \end{aligned}$$

OR

$$\begin{aligned}
 &\text{The value of } c \text{ should not exceed } 0.25b_f \\
 c &= (0.25) (8.99) = 2.25 \text{ in} \\
 &\text{Choose } c = 2 \text{ in}
 \end{aligned}$$

b) Calculate the effective plastic section modulus of the beam at the zone of

plastic hinging  $Z_{rbs}$  :

$$Z_{rbs} = Z_{xb} - 4(c) (t_f) (d_b - t_f)/2$$

$$Z_{rbs} = 200 - 2(2) (0.68) (23.9 - 0.68)$$

$$Z_{rbs} = 136.84 \text{ in}^3$$

c) Calculation of  $M_f$ 

$$M_f = M_{pr} + V_p X$$

$M_f$  = Plastic moment at the face of the column

$M_{pr}$  = Portable plastic moment at the hinges

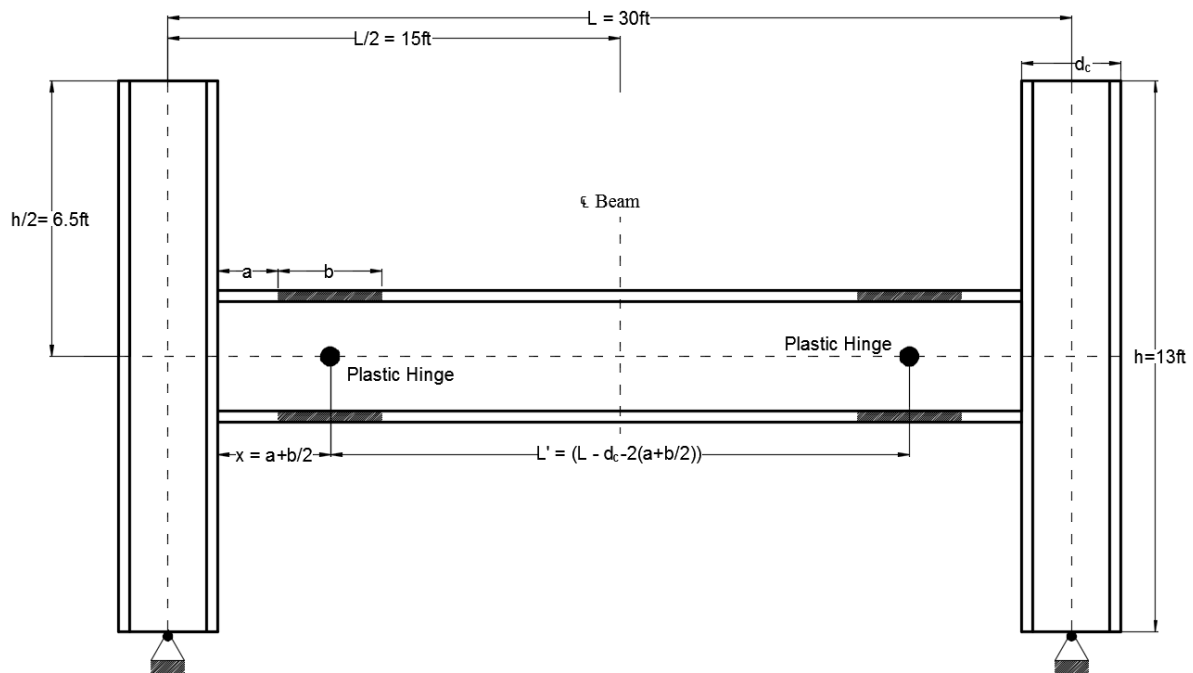


Figure A3: Plastic Hinge Formation for RBS

Calculation of Probable Plastic Moment at Hinges in reference to FEMA 350 and AISC Steel Construction Manual (AISC 2012)

$$M_{pr} = C_{pr} R_y Z_e F_y$$

$R_y$  = Coefficient, for A992 steel  $R_y = 1.1$

$C_{pr}$  = A factor to account for the peak connection strength, including strain hardening, local restraint, additional reinforcement, and other connection condition

$$C_{pr} = \frac{F_y + F_u}{2F_y} = \frac{50 + 65}{2(50)}$$

$$C_{pr} = 1.15$$

$$M_{pr} = (1.15)(1.1)(136.84)(50)$$

$$M_{pr} = 8655.13 \text{ k - in}$$

Calculate  $V_p$

Refer Figure A3

$$L' = L - d_c - 2(a+b/2)$$

$$L' = (2)(15)(12) - 15.2 - 2(6+10)$$

$$L' = 312.8 \text{ in}$$

$V_p$  = Shear at the plastic hinge

Assume that there are no gravitational forces

$$V_p = \frac{M_{pr}}{(L'/2)}$$

$$V_p = \frac{8655.13}{312.8/2}$$

$$V_p = 55.34 \text{ k}$$

Plastic hinge location from face of the column = X

$$X = a + (b/2)$$

$$= 6 + (20/2) = 16 \text{ in}$$

Calculate Moment at column face:

$$M_f = M_{pr} + V_p X$$

$$M_f = 8655.13 + (55.34)(16)$$

$$M_f = 9540.57 \text{ k - in}$$

d) Check for  $M_f < R_y Z_b F_y$

$$M_f < 1.1 \times 200 \times 50$$

$$M_f = 9540.57 \text{ k-in} < R_y Z_b F_y = 11000 \text{ k - in}$$

The design is acceptable

Step 3: Calculate  $M_c$  based on the final RBS dimensions:

$$M_c = M_{pr} + V_p (X + d_c/2)$$

$$M_c = 8655.13 + 55.34(16 + 15.2/2)$$

$$M_c = 9961.15 \text{ k - in}$$

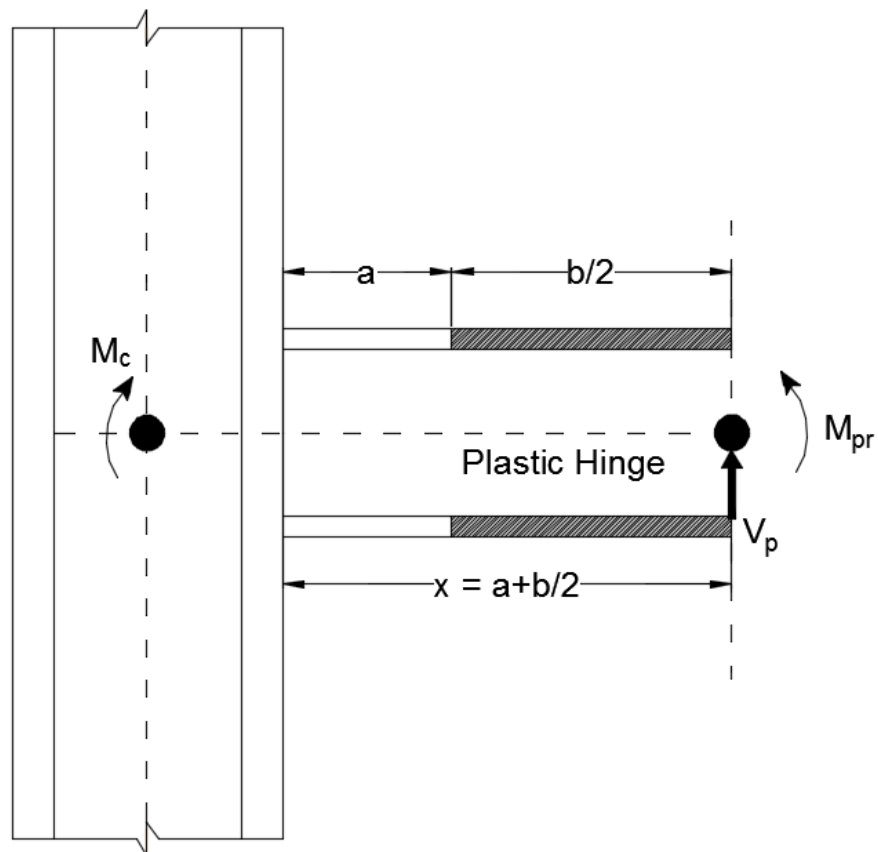


Figure A4: Calculation of moments at critical sections

Step 4: Calculate the shear at the column face  $V_f$

$$V_f = \left( \frac{2xM_f}{L-d_c} \right) + V_g$$

$V_g$  = Shear Force due to Gravity load

$$V_g = 0 \text{ k}$$

$$V_f = \frac{M_f}{\left( \frac{L}{2} \right) - \left( \frac{d_c}{2} \right)} + V_g$$

Assume that there is no gravity load on the beam  $V_g = 0$ , therefore

$$V_f = \frac{9540.57}{(15 \times 12) - \left( \frac{15.2}{2} \right)} + 0$$

$$V_f = 55.34 \text{ k}$$

Step 5: Design of Panel Zone Strength

Step-I: Calculate  $t$ , thickness of the panel zone

$$t = \frac{C_y M_c \left( \frac{h - d_b + t_{fb}}{h} \right)}{(0.9) 0.6 F_{yc} R_{yc} d_c (d_b - t_{fb})} \quad \text{Eq. (1)}$$

$h$  = the average story height of the stories above and below the panel zone.

$$h = 13 \text{ ft} = 156 \text{ in}$$

$R_{yc}$  = the ratio of the expected yield strength of the column material to the minimum specified yield strength in reference to Seismic Provisions for Structural Steel Buildings (AISC 2016).

$$R_{yc} = 1.1$$

$$C_y = \frac{1}{C_{Pr} \frac{Z_{rbs}}{S_{rbs}}}$$

$S_{rbs}$  = the elastic section modulus of the beam at the zone of plastic hinging

$Z_{rbs}$  = the effective plastic section modulus of the beam at the zone of plastic hinging

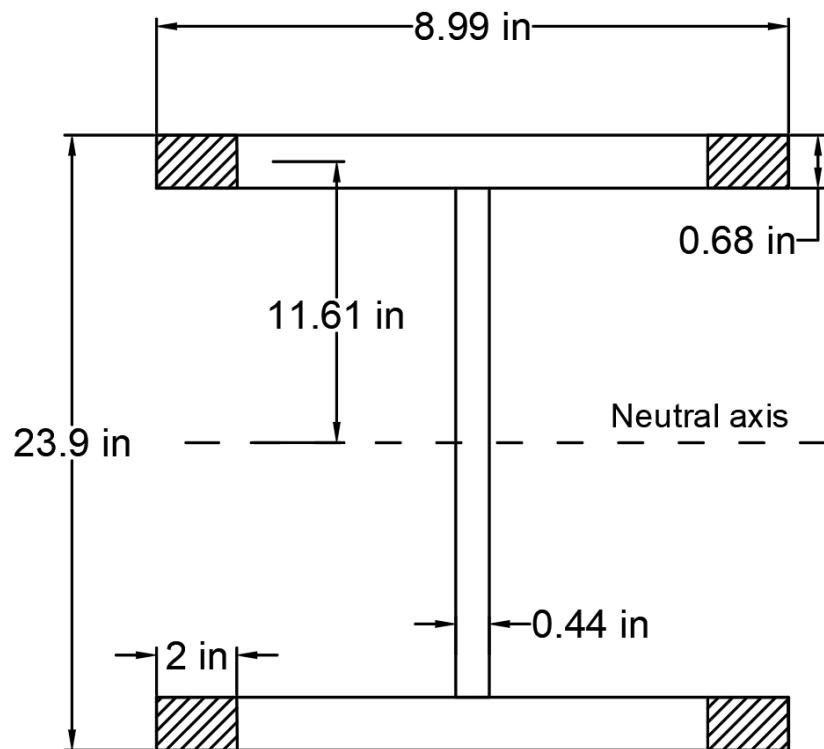


Figure A5: Calculation of Section modulus for RBS

Moment of Inertia of Reduced Beam Section ( $I_{rbs}$ ) =  $(L)(B^3)/12$

$$I_{rbs} = (2)(0.68^3)/12$$

$$I_{rbs} = 0.052 \text{ in}^3$$

$I_{rbs}$  about Neutral Axis =  $I_{rbs} + ((\text{Area})(d^2))$

$$I_{rbs} \text{ about Neutral Axis} = 0.052405 + ((2)(0.68)(11.61^2))$$

$$I_{rbs} \text{ about Neutral Axis} = 183.37 \text{ in}^3$$

Total  $I_{rbs}$  about Neutral Axis =  $(4)(183.37)$

$$\text{Total } I_{rbs} \text{ about Neutral Axis} = 733.68 \text{ in}^3$$

$S_{rbs}$  (Section Modulus for rectangle blocks) =  $(\text{Total } I_{rbs})/y$

$$S_{rbs} = \frac{733.48}{(23.9/2)}$$

$$S_{rbs} \text{ (only rectangle blocks)} = 61.37 \text{ in}^3$$

$S_{rbs}$  (I section) =  $S_{XX} - 61.37$

$$S_{rbs} \text{ (I section)} = 114.41 \text{ in}^3$$

$$C_y = \frac{1}{1.15 \left( \frac{136.84}{114.41} \right)}$$

$$C_y = 0.73$$

From Eq. (1) calculation of t:

$$t = \frac{0.73(9961.15) \left( \frac{156 - 23.9 - 0.68}{156} \right)}{(0.9)(0.6)(50)(1.1)(15.2)(23.9 - 0.68)}$$

$$t = 0.59 \text{ in}$$

Step-II: Check, if thickness of the panel zone 't' is greater than the thickness of the column web 't<sub>cw</sub>', provide the Doubler Plate or increase the column size to a section with adequate web thickness.

$$t < t_{wc}$$

$$t = 0.59 \text{ in} < t_{wc} = 0.83 \text{ in}$$

Required thickness of the panel zone is less than the thickness of the column web, so Doubler Plates are not required.

Step 6: Check for continuity plate requirements

Moment-resisting connections should be provided with beam flange continuity plates across the column web when the thickness of the column flange is less than the value given by either of the both equations mentioned below,

$$t_{cf} < 0.4 \sqrt{1.8 b_f t_f \frac{F_{yb} R_{yb}}{F_{yc} R_{yc}}}$$

Or

$$t_{cf} < \frac{b_f}{6}$$

Where:

t<sub>cf</sub> = minimum required thickness of column flange when no continuity plates are provided, inches

$b_f$  = beam flange width, inches

$t_f$  = beam flange thickness, inches

$F_{yb}$  ( $F_{yc}$ ) = Minimum specified yield stress of the beam (column) flange, ksi

$R_{yb}$  ( $R_{yc}$ ) = The ratio of the expected yield strength of the beam (column) material to the minimum specified yield strength from Seismic Provisions for Structural Steel Buildings (AISC 2016).

$$t_{cf} \leq 0.4 \sqrt{(1.8)(8.99)(0.68) \left( \frac{50 \cdot 1.1}{50 \cdot 1.1} \right)}$$

$$t_{cf} \leq 1.33 \text{ in}$$

Check whether  $t_{cf} \leq$  Above value

$$t_{cf} = 1.31 \text{ in} \leq 1.33 \text{ in}$$

Continuity plates are required

Or

$$t_{cf} < b_f / 6$$

$$t_{cf} = 1.31 \text{ in} < b_f / 6 = (8.99/6) = 1.49 \text{ in}$$

Continuity plates are required.

## Step 7: Lateral Load Calculations

$$M_c = 9961.15 \text{ k-in}$$

$$M_c = 830.1 \text{ k-ft}$$

$$\text{Lateral Load} = V_c$$

$$h = 13 \text{ ft}$$

$$M_c = V_c h = 830.11 \text{ k-ft}$$

$$V_c = \frac{830.11 \text{ k-ft}}{13 \text{ ft}}$$

$$V_c = 63.85 \text{ k}$$

$$\text{Lateral load} = 63.85 \text{ kips}$$

## VITA

Graduate School  
Southern Illinois University

Venkat Ramana Reddy Vootukuri

[ramana.vootukuri@gmail.com](mailto:ramana.vootukuri@gmail.com)

Gokaraju Rangaraju Institute of Engineering and Technology  
Bachelor of Technology, Civil Engineering, May 2016

Special Honors and Awards:

- Illinois Asphalt Pavement Association (IAPA) Scholarship Recipient for 2017-2018 school year
- Graduate Civil Engineering Departmental Scholarship (GSP) Recipient for 2017-2018 school year
- Higher Achievers Alternate Tuition Rate Award (For Entire Master's Degree)

Thesis Paper Title:

Comparison of Strength, Ductility and Stiffness for Radius Cut and Straight Cut of Reduced Beam Section

Major Professor: J. Kent Hsiao, Ph.D., P.E.(CA), S.E.(UT)

Publications:

1. T. Srinivas; V. Venkat Ramana Reddy; N V Ramana Rao (2016). EXPERIMENTAL INVESTIGATION ON STRENGTH PROPERTY OF LOW CALCIUM FLY ASH BASED GEOPOLYMER CONCRETE. International Conference on Smart Sustainable Cities (ICSSC - 2016),137-149 Retrieved from <http://www.elkjournals.com/>